against restenosis. Transfection of the DNAzyme into the arterial wall *in vivo* is difficult compared to transfection of DNA oligodeoxynucleotides (ODNs).[15] We and others previously demonstrated that *cis*-element 'decoy' ODNs of the transcription factor-binding site can be successfully transfected using an intraluminal approach and is effective in blocking the activity of several transcription factors.[15–17] Although there is no ideal experimental model available, the hypercholesterolemic rabbit model might be more relevant and appropriate for studying the usefulness of novel approaches against human restenosis.

Therefore, the primary aim of the present study was to test the hypothesis that blockade of Egr-1 activity reduces neointimal formation after balloon injury by inhibiting Egr-1-dependent proliferative-inflammatory changes in hypercholesterolemic rabbits. To achieve effective blockade of Egr-1 *in vivo*, we utilized transfection of synthetic double-stranded Egr-1 decoy ODNs. This decoy strategy involves the intracellular delivery of 'decoy' ODNs, which are then bound by Egr-1. Occupation of the Egr-1 DNA-binding site by the decoy ODN renders the protein incapable of binding to the promoter regions of the target genes.

Results

Egr-1 expression and activity in a balloon-injured artery

Egr-1 mRNA was not detectable in normal noninjured artery. Egr-1 mRNA expression had biphasic changes; an early and rapid rise at 1 h, a spontaneous decline at 6 and 24 h, reinduction at 7 and 28 days after injury (Figure 1a). Immunohistochemical staining revealed increased Egr-1 protein levels in the medial cells at the early phase and in neointimal and medial cells at the later phase after balloon injury (Figure 1b). To identify which cell types upregulate Egr-1, we performed double immunostaining (Figure 1c). We found that immunoreactive Egr-1 located in monocytes/macrophages and smooth muscle cells in the media at the early phase of day 7, and in neointimal and medial vascular smooth muscle cells at later phase of day 28. Egr-1 was also present in the endoluminal endothelial cells on day 28.

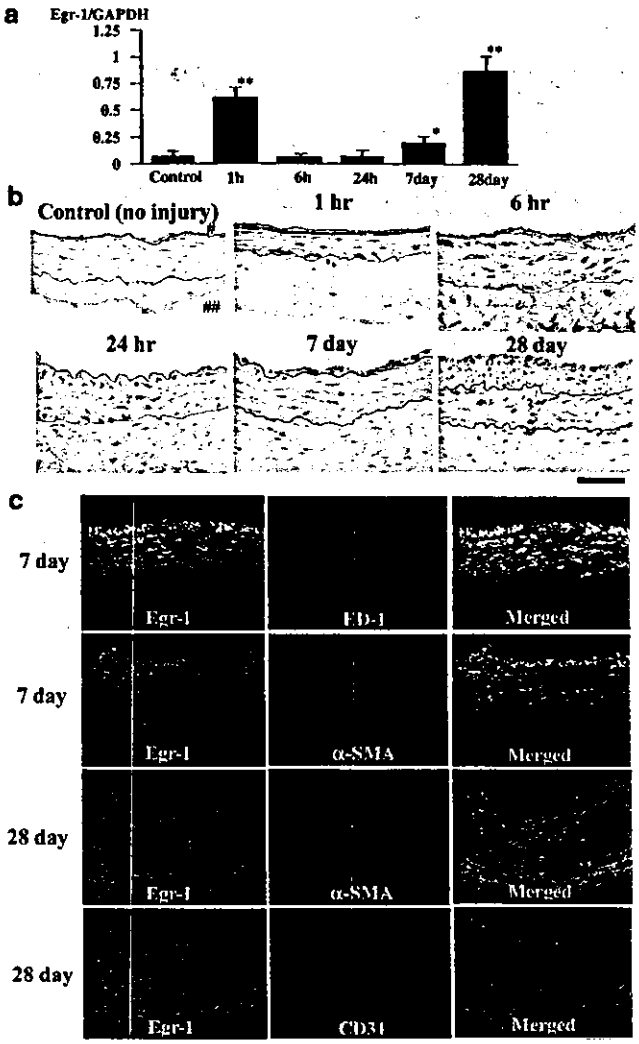

*Figure 1 Time course of Egr-1 gene and protein expression in the carotid artery after balloon injury. (a) Time course of Egr-1 gene expression by quantitative real-time PCR. *$P<0.05$, **$P<0.01$ versus noninjured normal control artery. (b) Immunohistochemical micrographs of rat carotid arteries after balloon injury stained for Egr-1. # and ## indicate the lumen and adventitia, respectively. Internal and external elastic layers are highlighted with blue and black lines, respectively. The bar indicates 50 μm. (c) Fluorescence double immunohistochemistry of rat carotid arteries after balloon injury. Micrographs of injured arteries are stained with Egr-1 in green. Micrographs of injured arteries are also stained with ED-1, α-SMA, or PECAM(CD31) in red. Single fluorescence-positive cells were stained in green or red, whereas double-positive cells were stained in yellow. The bar indicates 50 μm.*

Transfection of FITC-labeled Egr-1 decoy into the artery

Transfection of fluorescein-isothiocyanate (FITC)-ODNs resulted in widespread fluorescence in the medial layer of the injured arterial wall (Figure 2a). The transfection efficacy (percent of FITC-stained nuclei per total nuclei) was $6.2 \pm 1.6\%$.

Gel mobility-shift assay revealed that the Egr-1-binding activity was markedly increased compared with that of normal noninjured artery (Figure 2b). Complete competition of the increased Egr-1-binding activity by an excess Egr-1 decoy was observed. The increased Egr-1-binding activity was markedly diminished in the artery transfected with the Egr-1 decoy, but not in the artery transfected with the scrambled decoy ODN (Figure 2b).

Inhibitory effects of the Egr-1 decoy transfer on neointimal hyperplasia

On day 7, we detected RAM-11-positive monocytes and Ki-67-positive proliferating cells mainly in the media (Figure 3a). There was markedly less inflammation (RAM11-positive cells) and proliferation (Ki-67-positive cells) in Egr-1 decoy-transfected arteries than in untreated and scrambled decoy-transfected arteries (Figure 3b).

On day 28, thickened neointima was formed in the balloon-injured artery of all three groups (Figure 4a). Quantitative analysis demonstrated a significant reduction of the intima/media ratio in Egr-1 decoy-transfected arteries compared with the other two groups (Figure 4c). Endothelial cell linings, monitored by CD31

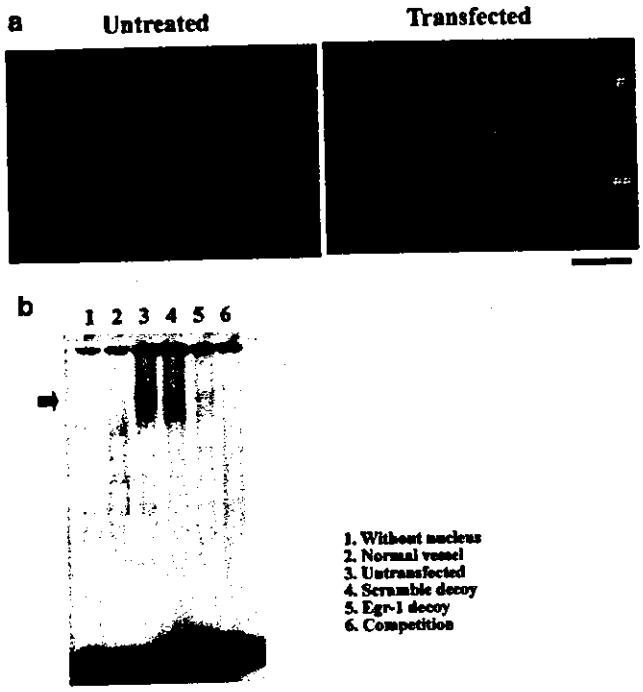

Figure 2 Inhibition of Egr-1 DNA-binding activity by Egr-1 decoy transfection in balloon-injured artery. (a) FITC-labeled decoy ODN transfection into the balloon-injured rabbit carotid artery. Weak background fluorescence is observed in elastic layers of untreated and transfected arteries. Spindle-shaped fluorescence staining, suggesting nuclear fluorescence in the transfected cells. The nuclear fluorescence-stained cells locate mainly in cells in the media. # and ## indicate the lumen and adventitia, respectively. The bar indicates 50 μm. (b) Gel mobility-shift assay for Egr-1-binding site. Lane 1, negative control (^{32}P-labeled Egr-1 decoy ODN without nuclear extract); lane 2, normal artery; lane 3, untreated balloon-injured artery; lane 4, balloon-injured artery transfected with scrambled decoy ODN; lane 5, balloon-injured artery transfected with Egr-1 decoy ODN; lane 6, balloon-injured artery transfected with Egr-1 decoy ODN incubated with extra amount of cold Egr-1 ODN. The arrow indicates migration of the band corresponding to Egr-1–DNA complex. These experiments were repeated five times, all with representative results.

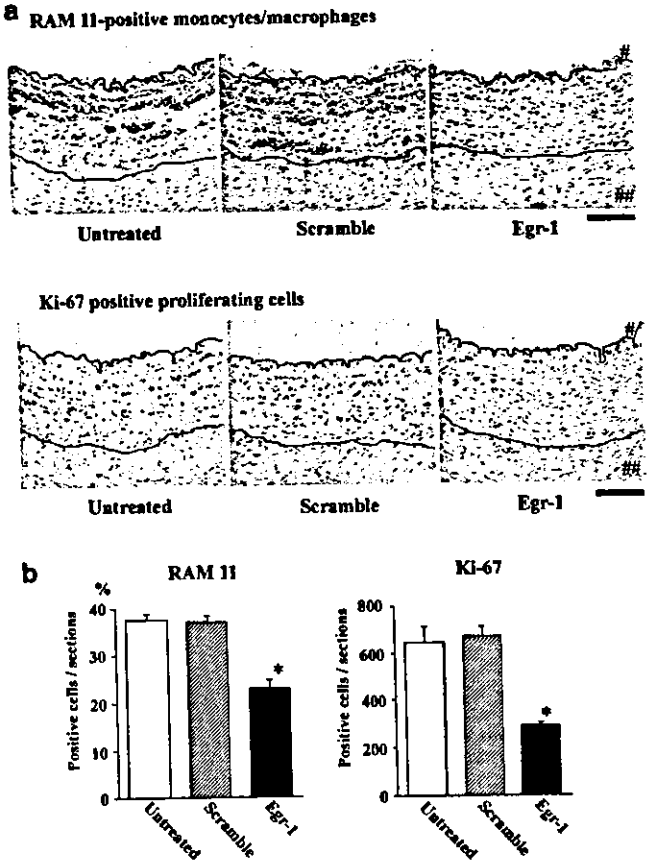

*Figure 3 Inhibitory effect of Egr-1 decoy transfection on early inflammatory and proliferative changes. (a) Carotid artery sections from the untreated group, scrambled group, and Egr-1 group 7 days after injury were stained immunohistochemically with the antibody against monocyte/macrophage (RAM11) or proliferating cells (Ki-67). # and ## indicate the lumen and adventitia, respectively. Bar=100 μm. (b) Effect of the Egr-1 decoy transfection on inflammation (RAM11-positive monocyte/macrophage) and proliferation (Ki-67 positive cells) 7 and after balloon-induced injury (n=8 each). *P<0.05 versus the untreated group.*

immunoreactivity, were observed equally in the three groups (Figure 4a).

Inhibitory effects of Egr-1 decoy transfer on expression of target genes

Egr-1 decoy transfection, but not scrambled decoy transfection, reduced the increased expression of PDGF-B, TGF-β1, and MCP-1 (Figure 5a). Egr-1 decoy transfection did not affect increased gene expression of interleukin (IL)-1β and TF. Immunohistochemical staining performed 7 days after balloon injury revealed increased immunoreactive PDGF-B, TGF-β1, and MCP-1 in cells in the neointima, and smooth muscle cells in the media (Figure 5b). Increases in PDGF-B, TGF-β1, and MCP-1 immunostaining were not observed in Egr-1 decoy-transfected arteries.

Plasma lipoprotein levels

There was no significant difference in the time course of plasma levels of low-density lipoprotein cholesterol among the three groups. The low-density lipoprotein cholesterol levels before and 28 days after injury were 452±47 and 471±63 mg/dl in the untreated group, 491±42 and 507±35 mg/dl in the scrambled decoy-transfected group, and 474±32 and 538±44 mg/dl in Egr-1 decoy-transfected group.

Discussion

Blockade of Egr-1 activation using the 'decoy' strategy attenuated early inflammation and proliferation and thus reduced later neointimal hyperplasia in balloon-injured arteries of hypercholesterolemic rabbits, suggesting that Egr-1 is an important target for restenosis. This study is the first to demonstrate the efficacy of Egr-1 decoy ODN transfection *in vivo* for restenosis therapy.

The most important finding in the present study is that blockade of Egr-1 activity by transfection of Egr-1 decoy ODN attenuated neointimal hyperplasia associated with the inhibition of inflammation (infiltration of RAM11-positive macrophages) and proliferation (appearance of proliferating cells). Also, Egr-1 decoy ODN transfection inhibited increased expression of Egr-1-dependent genes such as PDGF-B and TGF-β1 after balloon injury. Egr-1 decoy ODN transfection did not affect the expression of Egr-1-independent genes, such as IL-1β, suggesting specific inhibition of Egr-1-mediated gene transcription by Egr-1 decoy ODN transfection. Furthermore, there

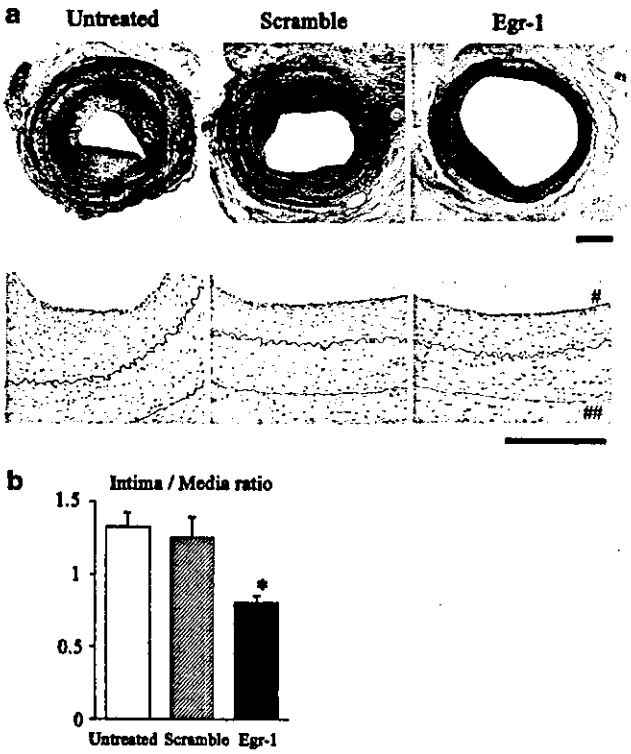

*Figure 4 Inhibitory effect of Egr-1 decoy transfection on neointimal hyperplasia. (a) Carotid artery sections 28 days after balloon-induced injury in untreated, scrambled decoy-transfected, and Egr-1 decoy-transfected arteries stained with elastic-van-Gieson (upper panels) or immunohistochemically for CD31 (lower panels). Internal and external elastic layers are highlighted with blue and black lines, respectively. Bar=200 μm. (b) Effect of the Egr-1 decoy transfection on the intima/media ratio 28 days after balloon injury (n=8 each). *P<0.05 versus the untreated and scrambled group.*

was increased immunoreactivity for PDGF-B, TGF-β1, and MCP-1 in balloon-injured arterial wall and increased inhibition by Egr-1 decoy ODN transfection. Neointimal hyperplasia is inhibited by blocking PDGF,[18,19] TGF-β1,[20,21] or MCP-1.[22–24] Therefore, it is reasonable to consider that the mechanisms by which the Egr-1 decoy ODN transfection attenuates neointimal hyperplasia after balloon injury is by decreased expression and activity of these target genes.

We demonstrated direct *in vivo* evidence for specific activation (increased DNA-binding activity) of Egr-1 in the balloon-injured artery and effective suppression of Egr-1 activation by transfection of synthetic double-stranded Egr-1 decoy ODN. As we could not stain Egr-1 immunohistochemically in rabbit tissues with available antibodies, we performed immunohistochemical staining of Egr-1 in a rat model. Egr-1 expression after balloon injury is biphasic and Egr-1-expressing cells locate in monocytes/macrophages and smooth muscle cells in the media at early phases and in the neointimal and vascular smooth muscle cells in the media at late phases of balloon injury. Egr-1 is activated by multiple external stimuli (ie, mechanical injury, cytokines, growth factors) that might contribute to the pathogenesis of neointimal hyperplasia after injury; therefore, the present data suggest that Egr-1 also participates in the chronic process of neointimal hyperplasia. A recent report by McCaffrey *et al*,[11] who demonstrated persistent expression of Egr-1 in activated smooth muscle cells and endothelial cells in chronic stages of both experimental and human atherosclerosis, supports this notion.

A caveat in the interpretation of the present data is the partial inhibition of neointimal hyperplasia. This might be due to the limited transfection efficiency of naked decoy ODN. Therefore, technologies that enhance transfection efficiency (ie, HVJ-liposome method, new catheters for decoy delivery) should be used for 'decoy' strategies in clinical gene therapy.

In conclusion, our present data suggest that Egr-1 has an important role in the pathogenesis of neointimal hyperplasia after balloon injury in hypercholesterolemic rabbits. The inhibitory effects of the Egr-1 decoy are explained by the inhibition of vascular inflammation and proliferation through decreased expression and activity of Egr-1-dependent genes. These results suggest that gene therapy using *in vivo* transfection of an Egr-1 decoy might be a new therapeutic option against restenosis. Recent studies reported that transfection of decoy ODN for other transcription factors (nuclear factor-κB,[25] activator protein-1[26]) also reduced neointimal hyperplasia after injury, possibly through inhibitory effects different from those of Egr-1 decoy ODN transfection. A double decoy strategy that facilitates simultaneous suppression of two transcription factors, therefore, would be another novel approach for restenosis therapy.

Materials and methods

Egr-1 'decoy' oligonucleotides

A double-stranded phosphorothioate Egr-1 decoy ODN was synthesized. The Egr-1 decoy ODN sequence was: 5′-CCGAGAGCGGGGGCGAGCGTG-3′ annealed to 5′-CACGCTCGCCCCGCTCTCGG-3′; the sequence of the scrambled ODN, which included unrelated oligonucleotides, was 5′-GAGGCCGGCAGGTCGCGAGGG-3′ annealed to 5′-CCCTCGCGACCTGCCGGCCTC-3′. Egr-1 ODN labeled with FITC at the 5′ end of one strand was used for fluorescent microscopic analysis of ODN distribution after transfection.

Animal model of balloon injury

The present experiments were reviewed and approved by the Committee on Ethics on Animal Experiments, Kyushu University Faculty of Medicine, and according to the Guidelines of the American Physiologic Society. A part of this study was performed at the Kyushu University Station for Collaborative Research and the Morphology Core.

Male Japanese white rabbits weighing 2.7–3.2 kg were fed a high cholesterol diet containing 1% cholesterol and 3% peanut oil for 2 weeks. After anesthesia, the right common carotid artery was injured by three passages of an inflated 2F Fogarty catheter.[22] The sham operation involved simple ligation of the left external carotid artery without balloon injury. After the operation, all rabbits were fed the same high cholesterol diet. After balloon injury, rabbits were randomly divided into three groups: the untreated group (n=31) received no treatment, the scrambled group (n=31) underwent transfection of the scrambled decoy ODN at the balloon injury site,

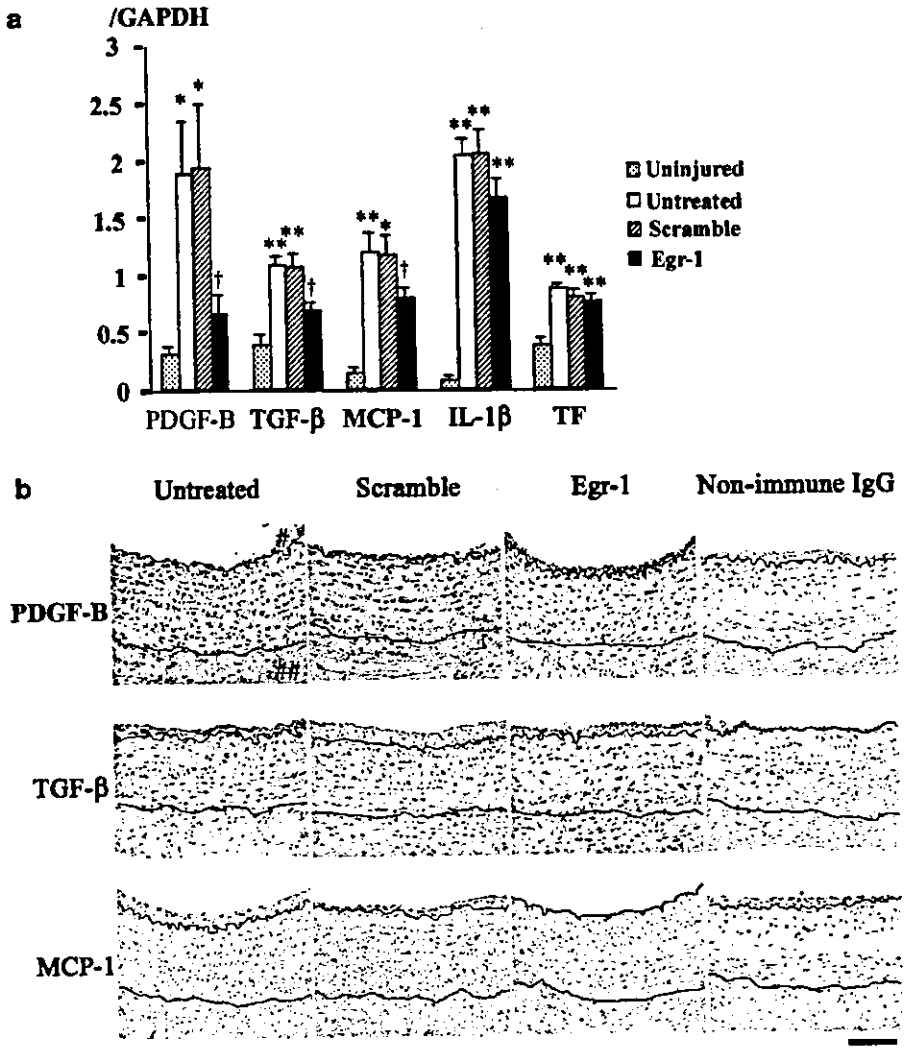

*Figure 5 Inhibitory effect of Egr-1 decoy transfection on the expression of target genes. (a) Effect of Egr-1 decoy transfection on mRNA levels of various genes. Quantitative real-time PCR was performed. *P<0.05, **P<0.01 versus uninjured control artery, †P<0.05 versus untreated and scrambled decoy-transfected artery. (b) Carotid artery sections from the untreated group, scrambled group, and Egr-1 group 7 days after balloon injury stained immunohistochemically with PDGF-B, TGF-β1 and MCP-1. Sections from the untreated group stained with nonimmune IgG are also presented. Internal and external elastic layers are highlighted with blue and black lines, respectively. Bar=100 μm.*

the Egr-1 group (n=33) underwent transfection of the Egr-1 decoy at the balloon injury site. Before insertion of the catheter, heparin (100 IU) was intravenously injected. For transfection of the decoy ODN, the pulse infusion catheter (Aishin Human Systems Co, Japan) was introduced into the injured common carotid artery site via the right external carotid artery immediately after balloon injury. A measure of 1 ml of the ODN solution (1 mg/1 ml, 80 μM) was infused via the catheter under a 300 mmHg pressure for 15 min. The infusion catheter was then removed and blood flow of the common carotid artery was re-established. At various time points after the operation, rabbits of each group were anesthetized and the injured or transfected common carotid arteries as well as the contralateral untransfected, unmanipulated carotid arteries were collected.

To determine the time course of Egr-1 protein expression, immunohistochemical staining for Egr-1 was performed in a rat model of carotid artery balloon injury. A rat model was used because the appropriate (rabbit Egr-1) antibody was not available. Male Wistar–Kyoto rats were anesthetized with sodium pentobarbital (50 mg/kg, i.p.) and balloon injury of the right common carotid artery was performed using an inflated 2F Fogarty balloon catheter,[23]

Analysis of FITC-ODNs

FITC-labeled ODN were instilled into the injured carotid arteries as above and the arteries were harvested 24 h after transfection. The efficacy of FITC-labeled ODN was assessed using a fluorescence microscope. Serial 5 μm cryosections of carotid arteries transfected with Egr-1 with FITC-labeled ODNs were prepared and recorded. Transfected cells were identified by enhancement of the fluorescein signal.

Electrophoretic mobility shift assay (EMSA)

The EMSA was performed on nuclear extracts prepared immediately from rabbit carotid arteries 2 h after injury using the method described previously.[17,27] Two carotid arteries were pooled so as to obtain one sample for one EMSA. Double-stranded ODN probes for Egr-1 (Santa

Cruz Biotechnology, Santa Cruz, CA, USA) were 5′-end labeled with [γ-^{32}P]dATP by using T4 polynucleotide kinase and standard procedures. For competition studies, a 100-fold molar excess of unlabeled probe for Egr-1 was added.

Histopathology and immunohistochemistry

The rabbit common carotid arteries were harvested, fixed with 10% paraformaldehyde or methacarn solution (methanol 60%; 1,1,1-trichloroethane 30%; and glacial acetic acid 10%). Sections were either stained with elastic-van Gieson stain or subjected to immunostaining. For immunohistochemistry, the slides were heated to induce epitope retrieval. To reduce nonspecific reactivity, sections were preincubated with 0.3% hydrogen peroxide and normal bovine serum. The primary antibodies used in the present study were as follows: mouse anti-rabbit macrophage antibody RAM11 (DAKO Co), the mouse anti-human Ki-67 antibody (DAKO Co), goat anti-human MCP-1 (R & D systems), mouse anti-human PDGF-B antibody PGF007 (Mochida Pharmaceutical Co), chicken anti-human TGF-β antibody (R & D Systems), or nonimmune IgG (Zymed).

The rat common carotid arteries were harvested, fixed with methacarn solution, embedded in paraffin, and cut into 5-μm thick sections. Sections were first stained with primary antibodies, rabbit anti-rat Egr-1 IgG (Santa Cruz Biotechnology), sequentially treated with a biotinylated species-specific secondary antibody, and stained with streptavidin-conjugated peroxidase substrate (Nichirei, Tokyo, Japan). The slides were counterstained with hematoxylin. Immunofluorescence double staining was performed to localize Egr-1 by the use of fluorescence-conjugated antibodies. The primary antibodies used in this study were mouse anti-rat ED-1 (Serotec), mouse α-smooth muscle actin (Dako), goat anti-PECAM (Santa Cruz).

Morphometric analysis

Morphometry and cell counting were performed by a single observer who was blind to the treatment protocols. To evaluate the neointimal thickening of the rabbit carotid arteries, the neointima to media ratio (*I/M* ratio) was measured using a computer-assisted analyzer (NIH Image).

Each tissue (four sections per artery) stained with RAM11 and Ki-67 was scanned. The number of positive cells in each section was determined. The sum of the immunopositive cells and the number of total cells in each section were counted. Then the percentage of immunopositive cells per total cells in each section was calculated, and the average of the four sections was reported for each animal.

Table 1 Probes used for real-time PCR

Assay	*Sequence*	*Acc. no.*
Egr-1		
Forward	5′-GCTTCCAGGTCCCCATGAT-3′	AJ291320
Reverse	5′-CCTTGATGGTGGAGAGTGGAG-3′	
TaqMan probe	5′-CCGACTACCTGTTTCCGCAGCA-3′	
PDGF-B		
Forward	5′-CCCATCTACATCATCACCGAGTAC-3′	AB020215
Reverse	5′-GAGTGCTGCTGCAGGAAGGT-3′	
TaqMan probe	5′-TGGACTACCTGCACCGCAACAAGC-3′	
TGF-β1		
Forward	5′-TGCTTCAGCTCCACAGAGAAGA-3′	AB020217
Reverse	5′-GGCAGAAGTTGGCGTGGTA-3′	
TaqMan probe	5′-TGTGCGGCAGCTGTACATTGACTTCC-3′	
MCP-1		
Forward	5′-TGAGCACGTTTCAGTGAGCAT-3′	M28883
Reverse	5′-ACCACACCTGCCTTTACACCTAA-3′	
TaqMan probe	5′-ATGAAGTCGTAGACCAGCAGCCCCC-3′	
IL-1β		
Forward	5′-TCAGCACCTCTCAGACAGAGTACAT-3′	M26295
Reverse	5′-AAGACACGAATTCCATGCTGAA-3′	
TaqMan probe	5′-AAACAACAGTGGCGGCCAAGACCTAA-3′	
TF		
Forward	5′-CACGGTGGCTCAGACATCAG-3′	M55390
Reverse	5′-CGTGCAAAAGGCACCGTAGT-3′	
TaqMan probe	5′-CGGTACAGCCAATCCCAGCTTGTTTC-3′	
GAPDH		
Forward	5′-CTCTGGCAAAGTGGATGTTGTC-3′	L23961
Reverse	5′-GGGTGGAATCATACTGGAACATG-3′	
TaqMan probe	5′-CCATCAATGATCCATTCATTGACCTCCA-3′	

Acc. no. indicates the accession number in GenBank.

Real-time reverse quantitative transcription-polymerase chain reaction

Real-time polymerase chain reaction (PCR) amplification was performed with the rabbits' cDNA using the ABI PRISM 7000 Sequence Detection System (Applied Biosystems) as described previously.[23] The respective PCR primers and TaqMan probes were designed from GenBank databases using a software program (Applied Biosystems; Table 1). The results were analyzed using the Sequence Detection Software (Applied Biosystems) and expressed in arbitrary units and adjusted for GAPDH mRNA levels.

Statistical analysis

Data are expressed as the mean ± s.e. Statistical analysis of differences was compared by the analysis of variance and Bonferroni's multiple comparison tests. A *P*-value of less than 0.05 was considered to be statistically significant.

Acknowledgements

This study was supported by Grants-in-Aid for Scientific Research (14657172, 14207036) from the Ministry of Education, Science, and Culture, Tokyo, Japan, by Health Science Research Grants (Comprehensive Research on Aging and Health, and Research on Translational Research) from the Ministry of Health Labor and Welfare, Tokyo, Japan, and by the Program for Promotion of Fundamental Studies in Health Sciences of the Organization for Pharmaceutical Safety and Research, Tokyo, Japan.

References

1 Ross R. Atherosclerosis – an inflammatory disease. *N Engl J Med* 1999; **340**: 115–126.
2 Lusis AJ. Atherosclerosis. *Nature* 2000; **407**: 233–241.
3 Glass CK, Witztum JL. Atherosclerosis. The road ahead. *Cell* 2001; **104**: 503–516.
4 Libby P, Ganz P. Restenosis revisited – new targets, new therapies. *N Engl J Med* 1997; **337**: 418–419.
5 Topol EJ, Serruys PW. Frontiers in interventional cardiology. *Circulation* 1998; **98**: 1802–1820.
6 Morice MC *et al*. A randomized comparison of a sirolimus-eluting stent with a standard stent for coronary revascularization. *N Engl J Med* 2002; **346**: 1773–1780.
7 Sousa JE *et al*. Sustained suppression of neointimal proliferation by sirolimus-eluting stents: one-year angiographic and intravascular ultrasound follow-up. *Circulation* 2001; **104**: 2007–2011.
8 Khachigian LM, Collins T. Inducible expression of Egr-1-dependent genes. A paradigm of transcriptional activation in vascular endothelium. *Circ Res* 1997; **81**: 457–461.
9 Khachigian LM, Lindner V, Williams AJ, Collins T. Egr-1-induced endothelial gene expression: a common theme in vascular injury. *Science* 1996; **271**: 1427–1431.
10 Khachigian LM. Catalytic DNAs as potential therapeutic agents and sequence-specific molecular tools to dissect biological function. *J Clin Invest* 2000; **106**: 1189–1195.
11 McCaffrey TA *et al*. High-level expression of Egr-1 and Egr-1-inducible genes in mouse and human atherosclerosis. *J Clin Invest* 2000; **105**: 653–662.
12 Kim S *et al*. Angiotensin II type 1 receptor blockade inhibits the expression of immediate-early genes and fibronectin in rat injured artery. *Circulation* 1995; **92**: 88–95.
13 Santiago FS *et al*. New DNA enzyme targeting Egr-1 mRNA inhibits vascular smooth muscle proliferation and regrowth after injury. *Nat Med* 1999; **5**: 1438.
14 Lowe HC *et al*. Catalytic oligodeoxynucleotides define a key regulatory role for early growth response factor-1 in the porcine model of coronary in-stent restenosis. *Circ Res* 2001; **89**: 670–677.
15 Morishita R, Higaki J, Tomita N, Ogihara T. Application of transcription factor 'decoy' strategy as means of gene therapy and study of gene expression in cardiovascular disease. *Circ Res* 1998; **82**: 1023–1028.
16 Mann MJ, Dzau VJ. Therapeutic applications of transcription factor decoy oligonucleotides. *J Clin Invest* 2000; **106**: 1071–1075.
17 Kitamoto S *et al*. Increased activity of nuclear factor-kappaB participates in cardiovascular remodeling induced by chronic inhibition of nitric oxide synthesis in rats. *Circulation* 2000; **102**: 806–812.
18 Yu JC *et al*. Efficacy of the novel selective platelet-derived growth factor receptor antagonist CT52923 on cellular proliferation, migration, and suppression of neointima following vascular injury. *J Pharmacol Exp Ther* 2001; **298**: 1172–1178.
19 Deguchi J *et al*. Targeting endogenous platelet-derived growth factor B-chain by adenovirus-mediated gene transfer potently inhibits *in vivo* smooth muscle proliferation after arterial injury. *Gene Therapy* 1999; **6**: 956–965.
20 Yamamoto K *et al*. Ribozyme oligonucleotides against transforming growth factor-beta inhibited neointimal formation after vascular injury in rat model: potential application of ribozyme strategy to treat cardiovascular disease. *Circulation* 2000; **102**: 1308–1314.
21 Smith JD *et al*. Soluble transforming growth factor-beta type II receptor inhibits negative remodeling, fibroblast transdifferentiation, and intimal lesion formation but not endothelial growth. *Circ Res* 1999; **84**: 1212–1222.
22 Mori E *et al*. Essential role of monocyte chemoattractant protein-1 in development of restenotic changes (neointimal hyperplasia and constrictive remodeling) after balloon angioplasty in hypercholesterolemic rabbits. *Circulation* 2002; **105**: 2905–2910.
23 Usui M *et al*. Anti-monocyte chemoattractant protein-1 gene therapy inhibits restenotic changes (neointimal hyperplasia) after balloon injury in rats and monkeys. *FASEB J* 2002; **16**: 1838–1840.
24 Egashira K *et al*. Importance of monocyte chemoattractant protein-1 pathway in neointimal hyperplasia after periarterial injury in mice and monkeys. *Circ Res* 2002; **90**: 1167–1172.
25 Yoshimura S *et al*. Inhibition of intimal hyperplasia after balloon injury in rat carotid artery model using *cis*-element 'decoy' of nuclear factor-kappaB binding site as a novel molecular strategy. *Gene Therapy* 2001; **8**: 1635–1642.
26 Kume M *et al*. Administration of a decoy against the activator protein-1 binding site suppresses neointimal thickening in rabbit balloon-injured arteries. *Circulation* 2002; **105**: 1226–1232.
27 Usui M *et al*. Important role of local angiotensin II activity mediated via type 1 receptor in the pathogenesis of cardiovascular inflammatory changes induced by chronic blockade of nitric oxide synthesis in rats. *Circulation* 2000; **101**: 305–310.

Critical Role of Monocyte Chemoattractant Protein-1 Receptor CCR2 on Monocytes in Hypertension-Induced Vascular Inflammation and Remodeling

Minako Ishibashi, Ken-ichi Hiasa, Qingwei Zhao, Shujiro Inoue, Kisho Ohtani, Shiro Kitamoto, Miyuki Tsuchihashi, Takeshi Sugaya, Israel F. Charo, Shinobu Kura, Teruhisa Tsuzuki, Tatsuro Ishibashi, Akira Takeshita, Kensuke Egashira

Abstract—Activated monocytes are present in the arterial walls of hypertensive patients and animals. Monocyte chemoattractant protein-1 (MCP-1), which controls monocyte function through its receptor (CCR2), is implicated in hypertensive inflammatory changes in the arterial wall. The role of CCR2 expression on monocytes in hypertension-induced vascular remodeling, however, has not been addressed. We hypothesized that CCR2 on monocytes is critical in hypertension-induced vascular inflammation and remodeling. Hypertension was induced by infusion of angiotensin II (Ang II) into wild-type mice, CCR2-deficient ($CCR2^{-/-}$) mice, and bone marrow-transferred mice with a leukocyte-selective CCR2 deficiency (BMT-$CCR2^{-/-}$). In wild-type mice, Ang II increased CCR2 intensity in circulating monocytes, which was prevented by an Ang II type-1 (AT_1) receptor blocker or blunted in AT_1 receptor–deficient mice. Enhanced CCR2 intensity on monocytes was observed in hypertensive patients and rats, and was reduced by treatment with the Ang II receptor blocker, supporting the clinical relevance of the observation in mice. In $CCR2^{-/-}$ and BMT-$CCR2^{-/-}$ mice, Ang II–induced vascular inflammation and vascular remodeling (aortic wall thickening and fibrosis) were blunted as compared with control mice. In contrast, Ang II–induced left ventricular hypertrophy developed in $CCR2^{-/-}$ and BMT-$CCR2^{-/-}$ mice. The present study suggests that CCR2 expression in monocytes has a critical role in vascular inflammation and remodeling in Ang II–induced hypertension, and possibly in other forms of hypertension. (*Circ Res.* 2004;94:1203-1210.)

Key Words: vascular remodeling ■ angiotensin II ■ inflammation ■ leukocytes

Chronic monocyte-mediated inflammation in arterial walls is observed in hypertensive patients and animals.[1–3] Recent clinical studies reported that lowering angiotensin II (Ang II) activity is a practical target of therapy for patients with cardiovascular disease.[4–6] Ang II mediates reactive oxidative species (ROS) and stimulates the release of cytokines and growth factors (interleukin-6) and the expression of adhesion molecules (vascular cell adhesion molecule-1) and chemokines [monocyte chemoattractant protein-1 (MCP-1)] that mediate arterial wall inflammation.[1–3] For example, Ang II can induce monocyte chemotaxis by producing MCP-1 from vascular smooth muscle cells and monocytes through NF-κB.[7,8]

MCP-1 is a C-C chemokine that controls monocyte recruitment to the site of inflammation through its receptor, C-C chemokine receptor (CCR) 2.[9–11] The MCP-1/CCR2 pathway appears to be involved in the inflammatory aspect of hypertensive artery disease. MCP-1 and CCR2 expression and activity are enhanced in the arterial walls of hypertensive animals.[12,13] Furthermore, activation of the MCP-1/CCR2 pathway induces monocyte-mediated inflammation, as well as production of adhesion molecules,[14] inflammatory cytokines,[15] and tissue factor,[16] and stimulates migration of vascular smooth muscle cells, resulting in neointimal hyperplasia or atherosclerosis.[17–20] We previously demonstrated that blockade of the MCP-1/CCR2 pathway prevents vascular inflammation and arteriosclerosis in rats made hypertensive by chronic inhibition of nitric oxide synthesis.[13,21–24] Blockade or abrogation of MCP-1 or CCR2 markedly attenuates the early development of atherosclerosis as well as the progression and destabilization of established lesions in hyperlipidemic mice.[25–28,29] CCR2-deficient ($CCR2^{-/-}$) mice display reduced neointimal formation after arterial injury.[24,30]

Original received September 22, 2003; resubmission received February 11, 2004; revised resubmission received March 22, 2004; accepted March 22, 2004.

From the Department of Cardiovascular Medicine (M.I., K.H., Q.Z., S.I., K.O., S. Kitamoto, M.T., A.T., K.E.) and Department of Medical Biophysics and Radiation Biology (S. Kura, T.T.), Department of Ophthalmology (T.I.), Graduate School of Medical Science, Kyushu University, Fukuoka, Japan; Discovery Research Laboratory (T.S.), Tanabe Seiyaku Co, Ltd, Kashima, Osaka, Japan; and Gladstone Institute of Cardiovascular Disease (I.F.C.), San Francisco, Calif.

Correspondence to Kensuke Egashira, MD, PhD, Department of Cardiovascular Medicine, Graduate School of Medical Science, Kyushu University, 3-1-1, Maidashi, Higashi-ku, Fukuoka 812-8582, Japan. E-mail egashira@cardiol.med.kyushu-u.ac.jp

Circulation Research is available at http://www.circresaha.org

DOI: 10.1161/01.RES.0000126924.23467.A3

Recently, Bush et al[31] reported that arterial hypertrophy induced by Ang II–induced hypertension was attenuated in $CCR2^{-/-}$ mice, suggesting that CCR2 is required for arterial hypertrophy induced in Ang II–induced hypertension. Most previous studies investigating the inflammatory aspects of hypertensive vascular disease, however, focused exclusively on stress- or injury-induced local changes in inflammation-driving factors in arterial wall cells. The functional importance of CCR2 expression on monocytes in hypertension-induced inflammation and vascular remodeling, on the other hand, has received little attention. Therefore, the present study tested the hypothesis that (1) CCR2 expressed in circulating monocytes is enhanced in hypertensive animals and patients via stimulation of Ang II type-1 (AT_1) receptors; and (2) CCR2 expressed on circulating monocytes has a critical role in hypertension-induced inflammation and vascular remodeling. To dissect the specific role of CCR2 in monocytes, we used bone marrow cells transplantation (BMT) techniques to create mice with a leukocyte-selective CCR2 deficiency (BMT-$CCR2^{-/-}$ mice) and demonstrated that Ang II–induced inflammation and vascular remodeling were blunted in BMT-$CCR2^{-/-}$ mice as well as in $CCR2^{-/-}$ mice.

Materials and Methods

Experimental Animals

Male wild-type mice (C57 BL/6J) and those overexpressing human superoxide dismutase (6-TgN(SOD1)3Cje) (SOD-TG) were purchased from Jackson Laboratory (Bar Harbor, Maine). Male AT_1a receptor–deficient mice (AT_1R-KO) on a C57BL/6J genetic background[32] were supplied from Tanabe Seiyaku Inc., Osaka, Japan. $CCR2^{-/-}$ and wild-type ($CCR2^{+/+}$) mice with the same genetic background (C57BL/6J and 129/svjae hybrids) were supplied from Dr Charo.[25] Male $CCR2^{-/-}$ and $CCR2^{+/+}$ mice were age matched for all experiments. All mice were bred and maintained in the Laboratory of Animal Experiments at Kyushu University. Twenty-week-old male Wistar-Kyoto (WKY) rats and 12-week-old spontaneous hypertensive rats (SHR) were obtained from an established colony at the animal Research Institution of Kyushu University, Faculty of Medical Sciences (Fukuoka, Japan).

Experimental Protocol

The study protocol was reviewed and approved by the Committee on the Ethics of Animal Experiments, Kyushu University Graduate School of Medical Sciences. A part of this study was performed at the Kyushu University Station for Collaborative Research and the Morphology Core Unit, Kyushu University Faculty of Medical Sciences.

Experiment 1

To examine whether Ang II affects CCR2 fluorescence intensity in circulating monocytes in vivo, Ang II was infused into several groups of 12-week-old wild-type mice treated with or without AT_1 receptor blocker (ARB), AT_1R-KO, or SOD-TG mice. The control group received untreated chow and drinking water. The Ang II group received Ang II via an osmotic minipump (Alzet) (1.9 mg/kg per day). The minipump was implanted in the peritoneal cavity under anesthesia with ketamine (80 mg/kg IP) and xylazine (10 mg/kg IP). The Ang II+ARB groups received Ang II by an osmotic minipump and ARB (olmesartan at 0.35 or 3.5 mg/kg per day) in chow. Olmesartan was a gift from Sankyo Pharmaceutical Co (Tokyo, Japan). Treatment with olmesartan was started 3 days before Ang II administration was begun. The AT_1R-KO+Ang II and SOD-TG+Ang II groups were infused with Ang II by osmotic minipumps.

Experiment 2

To determine the role of CCR2 in Ang II–induced vascular remodeling, four groups of 12-week-old $CCR2^{-/-}$ and $CCR2^{+/+}$ mice infused with Ang II or PBS via osmotic minipump were studied.

Experiment 3

To dissect the specific role of CCR2 in the monocytes, we used the BMT technique to create mice with a leukocyte selective CCR2 deficiency (BMT-$CCR2^{-/-}$). At 8 weeks of age, BMT was performed as described previously.[33] Bone marrow cells were harvested from femurs and tibias of either test ($CCR2^{-/-}$) or control ($CCR2^{+/+}$) donor mice. The recipient $CCR2^{+/+}$ mice received 1×10^7 bone marrow cells (0.3 mL) 4 hours after whole body irradiation with 7 Gy of X-rays (200 KVp, 20 mA, 0.3 mmCu filter) at 1Gy/min. These two groups of mice are referred to as BMT-$CCR2^{-/-}$ and BMT-$CCR2^{+/+}$, respectively. Four groups of BMT-$CCR2^{-/-}$ and BMT-$CCR2^{+/+}$ mice infused with Ang II or PBS were studied. BMT-AT_1R-KO mice also were created in a same manner. To ensure that the exposure dose was sufficient to ablate the bone marrow, a group of C57Bl/6J mice (n=6) was irradiated and injected with bone marrow cells from C57BL/6J mice expressing green fluorescence protein. Flow cytometric analysis of circulating leukocytes from recipient mice at 4 weeks after transplantation revealed that the chimerism was 95±2%.

Experiment 4

To examine the effect of ARB on monocyte CCR2 fluorescence intensity in other forms of hypertension, we used WKY rats treated with N^{ω}-nitro-L-arginine methyl ester (L-NAME) and SHR treated with or without ARB.

In all experiments, mice were euthanized on day 3, 7, or 28 of treatment for morphometric, immunohistochemical, and biochemical analysis. Venous blood was collected immediately before the mice were euthanized. The aortas and hearts were isolated and either fixed in 10% buffered formalin for histologic analysis or snap-frozen in liquid nitrogen and stored at −80°C for biochemical analysis. Systolic blood pressure was measured by the tail-cuff method before and 3, 7, and 28 days after treatment.

Histology and Immunohistochemistry

Histopathology and immunohistochemistry were performed as described previously.[24,28] Some sections were subjected to immunostaining using antibodies against mouse macrophages (Mac-3, Serotec Inc), proliferating cell nuclear antigen (PCNA, DAKO), α-smooth muscle cell actin (α-SM actin) (Boehringer Mannheim), MCP-1, and CCR2 (Santa Cruz Biotechnology Inc). The degree of vascular remodeling (the medial thickness and perivascular fibrosis of aorta) and left ventricular hypertrophy [left ventricular to body weight ratios (LV/BW)] on day 28 was measured as described previously.[23]

TaqMan Real-Time Reverse Transcription–Polymerase Chain Reaction Analysis

TaqMan real-time reverse transcription–polymerase chain reaction (RT-PCR) was performed as previously described.[18] Transcripts from 1 μg total RNA were reverse-transcribed and the resultant cDNA was amplified by TaqMan real-time RT-PCR. The PCR primers for mouse MCP-1, CCR2, and B-type natriuretic peptide (BNP) were sense primer 5′-CCTGGATCGGA-ACCAAATGA-3′, antisense primer 5′-CGGGTCAACTTCA-CATTCAAAG-3′, and probe oligonucleotides 5′- AACT-GCATCTGCCCTAAGG-TCTTCAGCA-3′ for MCP-1, and sense primer 5′-CCTTGGGA-ATGAGTAACTGTGTGAT-3′, antisense primer 5′-ATGGA-GAGATACCTTCGGAACTTCT-3′, and probe oligonucleotides 5′-CACTTAGACCAGGCCATGCAGGT-GACA-3′ for CCR2, and sense primer 5′-GCCAGTCTCCAG-AGCAATTCA-3′, antisense primer 5′-GTGAGGCCTTGG-TCCTTCAA-3′, and probe oligonucleotides 5′-TCTCTTATCA-GCTCCAGCAGCTTCTGCA-3′ for BNP. GAPDH probe was obtained from Applied Biosystems.

Flow Cytometry Analysis

Flow cytometry analysis was performed as described previously.[33] To determine CCR2 expression in monocytes, isolated leukocytes were stained using antibodies against phycoerythrin (PE)-conjugated anti-mouse monocyte (CD80) (Becton Dickinson Biosciences), goat anti-mouse CCR2 (Santa Cruz Biotechnology Inc), and FITC-conjugated mouse anti-goat IgG (Santa Cruz Biotechnology Inc.). To determine CCR2 fluorescence intensity in lymphocytes and neutrophils, leukocytes were also stained using antibodies against PE-conjugated anti-mouse CD11b (Mac-1), cy-chrome-conjugated anti-mouse T-cell receptorβ chain monoclonal antibody (Becton Dickinson Biosciences). In control experiments, FITC-conjugated nonspecific goat IgG was used to measure nonspecific binding. The fluorescent probe, 2',7',-dichlorofluorescein diacetate (DCFH-DA, Molecular Probes Inc), was used to detect intracellular ROS. Isolated leukocytes were stained using DCFH-DA and PE-conjugated anti-mouse CD80 for 30 minutes at 4°C. Stained cells were analyzed by FACSCalibur (Becton Dickinson Biosciences).

Peripheral Blood Mononuclear Cell Chemotaxis

Mouse mononuclear cells were purified by centrifugation on Lympholyte-M and were washed with RPMI 1640. Cell migration was measured in 96-well chemotaxis chambers (Neuro Probe Inc). MCP-1 in RPMI 1640 (25 ng/mL) was added to the lower and the isolated mononuclear cells (2×10^7) in the same medium to the upper wells. After incubation for 90 minutes at 37°C, the membrane was removed, washed on the upper side with PBS. Migrated cells were counted. All assays were performed in triplicate.

Plasma Measurements

Commercially available ELISA kits (Biosource International) were used to measure mouse MCP-1 according to the manufacturer's instructions.

Patient Studies

Patients with hypertension who had no other evidence of other cardiovascular disease, infectious disease, inflammatory disorders, connective tissue disease, or prior malignant tumor disease, were enrolled. The patients were divided into three groups: normotensive group (systolic/diastolic blood pressure <140/90 mm Hg), untreated essential hypertensive patients (systolic/diastolic blood pressure ≥140/90 mm Hg), and hypertensive patients treated solely with ARB (losartan, candesartan, and valsartan). Hypertensive patients treated with a combination of antihypertensive drugs were not enrolled. Written informed consent was obtained from all patients.

Blood samples were obtained from all patients in the fasting state. White blood cell count, C-reactive protein, and plasma lipid, as well as plasma MCP-1 (human MCP-1 ELISA kit, Biosource International) were measured. The fluorescence intensity of chemokine receptors on leukocytes (the MCP-1 receptor CCR2 on monocytes, the interleukin-8 receptor CXCR2 on neutrophils, and the RANTES receptor CCR1 on T cells, DAKO) also was assessed by flow cytometry.

There were no significant differences in age, body mass index, plasma lipid levels, white blood cell count, or smoking habit among groups (Table 1). Plasma concentrations of MCP-1 and C-reactive protein were lower in the ARB-treated group, although the difference was not statistically significant. As expected, systolic and diastolic blood pressure were significantly higher in untreated hypertensive patients than in normotensive control subjects. Blood pressure values were lower in hypertensive patients treated with ARB than in untreated hypertensive patients, although the difference was not statistically significant. Hypertensive patients treated with ARB had a significantly higher proportion of diabetes mellitus.

Statistical Analysis

Data are expressed as mean±SE. In animal studies, statistical analysis of differences was compared by ANOVA using Bonferroni's correction for multiple comparisons. In human studies, multiple logistic regression analysis was performed to identify significant independent predictors of the presence of hypertension. Odds ratio and 95% confidence intervals were calculated. A level of $P<0.05$ was considered statistically significant.

TABLE 1. Clinical and Biochemical Characteristics of Hypertensive Patients With and Without ARB Treatment and Normotensive Controls

Variables	Normotensive Controls n=40	Untreated HT n=30	HT Treated With ARB n=30
Age	55±12	63±8	59±11
Male, %	71.7	63.0	63.6
Smoking, %	23.9	40.7	37.3
Body mass index	23±3	24±4	23±3
Hypercholesterolemia, %	34.8	37.0	46.4
Diabetes, %	21.1	29.6	53.7*
Systolic BP, mm Hg	115±12	151±10*	143±17*
Diastolic BP, mm Hg	67±10	84±9*	81±10*
WBC, $\times10^3/\mu L$	5.5±1.6	5.9±1.6	5.4±2.0
Monocyte count, $\times10^3/\mu L$	314±116	302±115	262±122
Total cholesterol, mg/dL	205±43	203±36	216±37
Triglycerides, mg/dL	120±57	119±50	142±53
LDL-C, mg/dL	112±33	108±34	114±21
C-reactive protein, mg/dL	0.13±0.4	0.17±0.3	0.10±0.3
MCP-1, pg/mL	11±6	13±10	9±6
CCR2 in monocytes, MFI	115±32	168±37*	111±24†
CXCR2 in neutrophils, MFI	85±35	77±25	81±16
CCR1 on T cells, MFI	10±3	11±3	10±3

Values are mean±SEM. *$P<0.01$ vs normotensive controls, †$P<0.01$ vs untreated hypertensive patients (HT).

Results

Ang II–Induced Upregulation of CCR2 in Circulating Monocytes in Wild-Type Mice

Flow-cytometry analysis indicated that monocyte CCR2 intensity peaked on day 7 and the higher level was sustained until day 28 of Ang II infusion (Figure 1A). The Ang II–induced increase in CCR2 intensity on day 7 was prevented by treatment with low and high doses of ARB. The Ang II–induced increase in CCR2 intensity was blunted in AT_1R-KO, SOD-TG, and BMT-AT_1R-KO mice (Figure 1B). No CCR2 antigen was detected on lymphocytes or neutrophils in the presence or absence of Ang II infusion. To determine the functional role of the CCR2 upregulation in monocytes, chemotaxis assay was performed in peripheral blood mononuclear cells. No chemotactic response was detected in monocytes from control untreated mice. In contrast, MCP-1–mediated chemotaxis was increased in monocytes from mice infused Ang II for 7 days, which was blunted in monocytes from $CCR2^{-/-}$ mice (Figure 1C). These chemotaxis data are in agreement with previous studies by other investigators[34,35] that the measured increase in CCR2 intensity on monocytes resulted in increased monocyte chemotaxis in response to MCP-1.

To study the effects of Ang II on intracellular ROS, intracellular ROS were measured in monocytes by

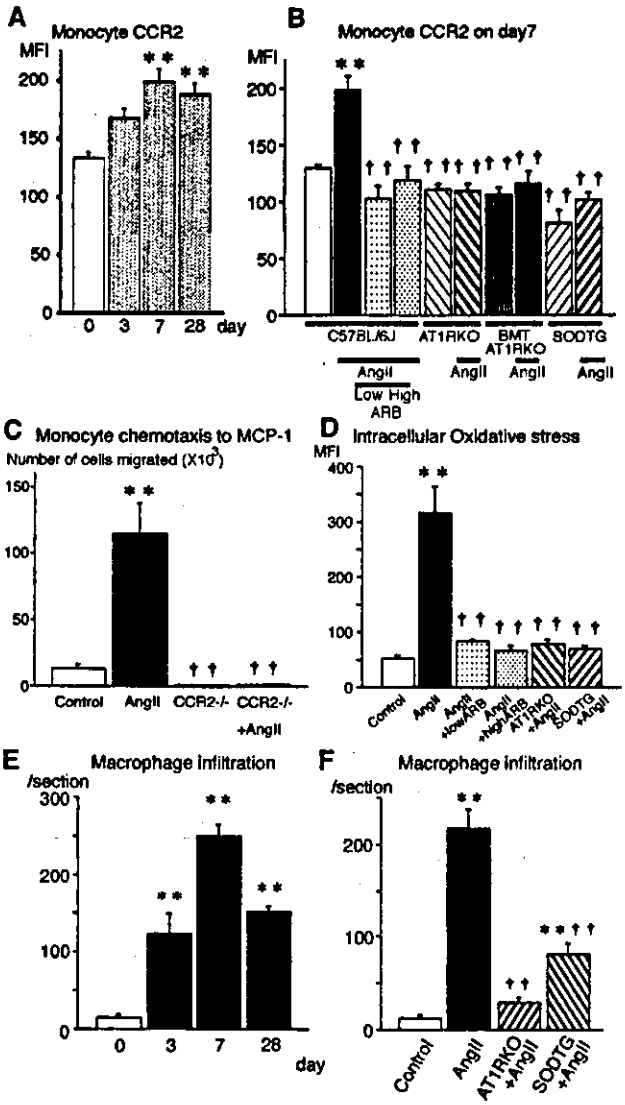

Figure 1. Ang II–induced CCR2 expression on circulating monocytes and macrophage infiltration into the aorta in wild-type mice. A, Time course of mean fluorescence intensity (MFI) of CCR2 on the surface of the circulating monocytes; n=6 to 8. B, Effects of ARB, AT_1 deficiency, leukocyte-selective AT_1R deficiency, and SOD overexpression on Ang II–induced enhancement of CCR2 expression on day 7; n=7 each. C, Effects of increased CCR2 expression on peripheral mononuclear cells chemotaxis in response to MCP-1 (25 ng/mL) in wild-type and $CCR2^{-/-}$ mice infused with or without Ang II for 7 days. D, Effects of ARB, AT_1 deficiency, and SOD overexpression on intracellular production of ROS in monocytes; n=6 each. E, Time course of macrophage infiltration after Ang II infusion (number of Mac-3–positive macrophages per section); n=6 each. F, Effect of ARB, AT_1 deficiency, and SOD overexpression on Ang II–induced macrophage infiltration into the aorta. Number of Mac-3–positive macrophages per section was determined on day 7; n=6 each. $^*P<0.05$, $^{**}P<0.01$ vs control group; $\dagger P<0.05$, $\dagger\dagger P<0.01$ vs Ang II group.

DCFH-DA fluorescence intensity (Figure 1D). Levels of ROS were undetectable in monocytes from untreated control mice, but were significantly increased in monocytes from mice infused with Ang II for 7 days. Treatment with the low and high doses of ARB prevented the increase in intracellular ROS. The Ang II–induced increase in ROS was blunted in AT_1R-KO and SOD-TG mice.

The time course of macrophages infiltration into the aorta was similar to that of monocyte CCR2 expression after Ang II infusion (Figures 1E and 1F). There was reduced Ang II–induced monocyte infiltration into the aorta in mice treated with low and high doses of ARB, AT_1R-KO, and SOD-TG mice.

Compared with the control group, Ang II infusion induced a rise in systolic blood pressure (online Table 1, available in the online data supplement at http://circres.ahajournals.org). Similar changes in blood pressure were observed in Ang II+Low ARB and SOD-TG+Ang II groups. No Ang II–induced increase in blood pressure was observed in the Ang II+High ARB and AT_1R-KO+Ang II groups (online Table 2). Baseline blood pressure was lower in AT_1R-KO mice, although the difference was not statistically significant.

Ang II–Induced Upregulation of MCP-1 and CCR2 in the Aorta in Wild-Type Mice

As previously reported,[12,31] Ang II infusion to wild-type mice for 7 days increased mRNA levels of MCP-1 and CCR2 (Figure 2A). Treatment with low and high doses of ARB prevented the increased gene expression. The Ang II–induced increase in gene expression was blunted in AT_1R-KO and SOD-TG mice. Immunohistochemical staining indicated that Ang II infusion increased MCP-1 in lesional macrophages on days 3 and 7, and the increase was sustained until day 28 (Figures 2B and 2C). Increased MCP-1 staining was noted in smooth muscle cells of the media on day 28. Increased CCR2 staining was observed in infiltrating macrophages on days 3, 7, and 28. Treatment with low and high doses of ARB prevented the Ang II–induced increase in immunostaining for MCP-1 and CCR2 (data not shown).

Inhibition of Ang II–Induced Vascular Remodeling in $CCR2^{-/-}$ Mice

As previously reported,[31] Ang II infusion to $CCR2^{+/+}$ mice for 7 days induced infiltration of Mac-3–positive macrophages into the aortic wall, mainly into the adventitia (Figure 3A). PCNA-positive proliferating cells appeared in cells in the endothelial layer, media, and adventitia. There were also α-SM actin–positive cells (myofibroblast) in the adventitia of Ang II–infused wild-type mice (data not shown). On day 28, aortic remodeling (medial wall thickening and perivascular fibrosis) developed in $CCR2^{+/+}$ mice. In contrast, aortic inflammatory-proliferative changes in the early stage and vascular remodeling in the late stage were markedly attenuated in $CCR2^{-/-}$ mice (Figure 3B).

There were no significant differences in plasma MCP-1 levels between untreated $CCR2^{+/+}$ and $CCR2^{-/-}$ mice on day 28 (online Table 2). In contrast, the plasma MCP-1 level dramatically increased in $CCR2^{-/-}$ mice infused with Ang II, compared with that in $CCR2^{+/+}$ mice infused with Ang II.

There were no significant differences in Ang II–induced changes in systolic blood pressure or left ventricular hypertrophy (online Table 2).

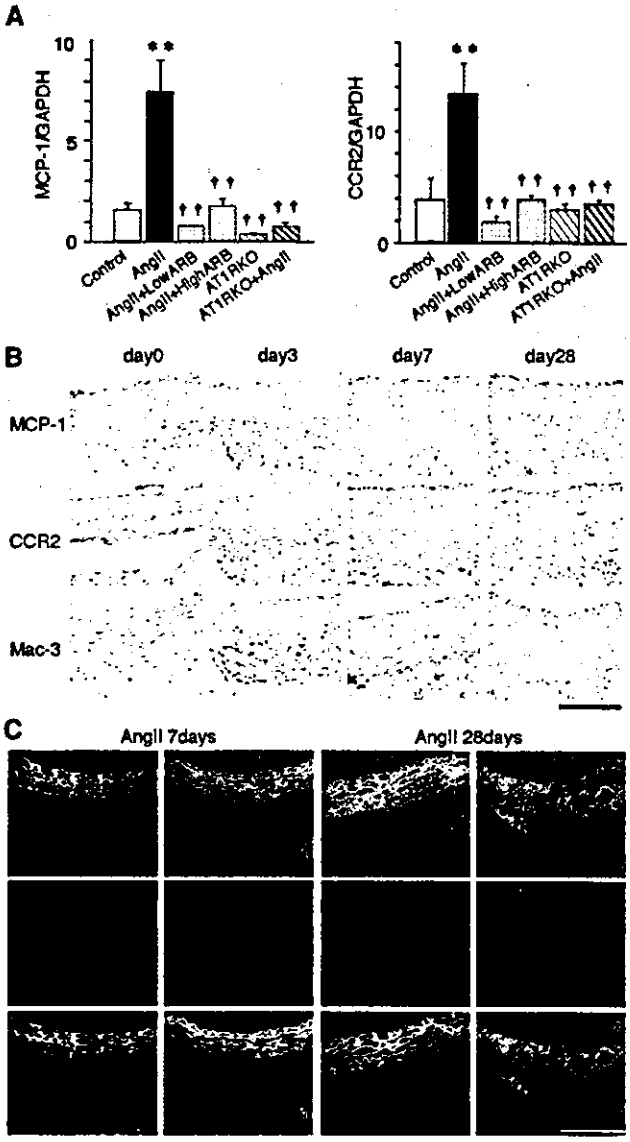

Figure 2. Ang II–induced expression of MCP-1 and CCR2 in the aorta in wild-type mice. A, MCP-1 and CCR2 gene expression by real-time RT-PCR in the aorta. Data are expressed as the ratio of MCP-1 and CCR2 mRNA to GAPDH mRNA. *$P<0.05$, **$P<0.01$ vs control group; †$P<0.05$, ††$P<0.01$ vs Ang II group; n=6 each. B, Aortic cross sections were stained immunohistochemically for MCP-1, CCR2, and macrophage (Mac-3) on days 0, 3, 7, and 28 (n=6 each) (bar=100 μm). C, Immunofluorescence double staining of aorta using anti-mouse CCR2, MCP-1, Mac-3, or α-SM actin antibody. CCR2 and MCP-1 immunofluorescence (labeled green with FITC), Mac-3 and α-SM actin immunofluorescence (labeled red with rhodamine), and their merged images (yellow) are presented. Background nonspecific fluorescence is observed in elastic layers of aortas (bar=100 μm).

Blunted Ang II–Induced Vascular Remodeling in BMT-CCR2$^{-/-}$ Mice

There were no differences in the degree of aortic wall thickening or perivascular fibrosis between untreated BMT-CCR2$^{+/+}$ and BMT-CCR2$^{-/-}$ mice. BMT-CCR2$^{+/+}$ mice developed significant vascular remodeling and left ventricular hypertrophy in response to Ang II infusion to an extent similar to that in nonirradiated CCR2$^{+/+}$ mice. In contrast, Ang II–induced aortic wall thickening and perivascular fibrosis were blunted in BMT-CCR2$^{-/-}$ mice (Figures 4A and 4B). There were no significant differences in Ang II–induced hypertension, left ventricular hypertrophy, or the increase in BNP mRNA levels between BMT-CCR2$^{+/+}$ and BMT-CCR2$^{-/-}$ mice (online Table 3).

As in nonirradiated CCR2$^{-/-}$ mice, there was a significant increase in plasma MCP-1 levels only in BMT-CCR2$^{-/-}$ mice infused with Ang II (online Table 3). Ang II–induced increases in MCP-1 mRNA and immunoreactive MCP-1 levels in the aorta were also similar between BMT-CCR2$^{+/+}$ and BMT-CCR2$^{-/-}$ mice (Figure 5). Aortic CCR2 gene expression was blunted in BMT-CCR2$^{-/-}$ mice infused with and

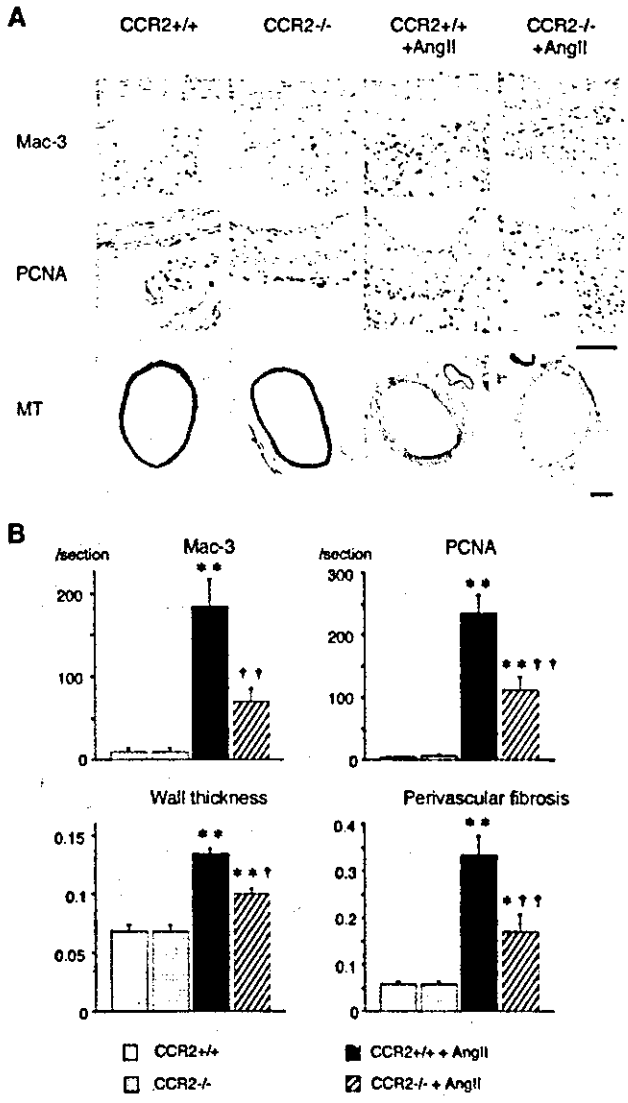

Figure 3. Inhibition of Ang II–induced inflammation and vascular remodeling in CCR2$^{-/-}$ mice. A, Aortic cross sections were immunohistochemically stained for macrophages (Mac-3) or a marker of proliferation (PCNA) on day 7. Aortic sections stained with Masson's trichrome on day 28 are also shown (bar=100 μm). B, Number of macrophages infiltrated into the aorta and appearance of proliferating cells in the CCR2$^{+/+}$, CCR2$^{-/-}$, CCR2$^{+/+}$+Ang II, and CCR2$^{-/-}$+Ang II mice on day 7 of Ang II infusion are shown (positive cell counts per section). Wall thickness (wall-to-lumen ratio) and perivascular fibrosis of aorta on day 28 are shown. *$P<0.05$, **$P<0.01$ vs CCR2$^{+/+}$ group; †$P<0.05$, ††$P<0.01$ vs CCR2$^{+/+}$+Ang II group (n=6 each).

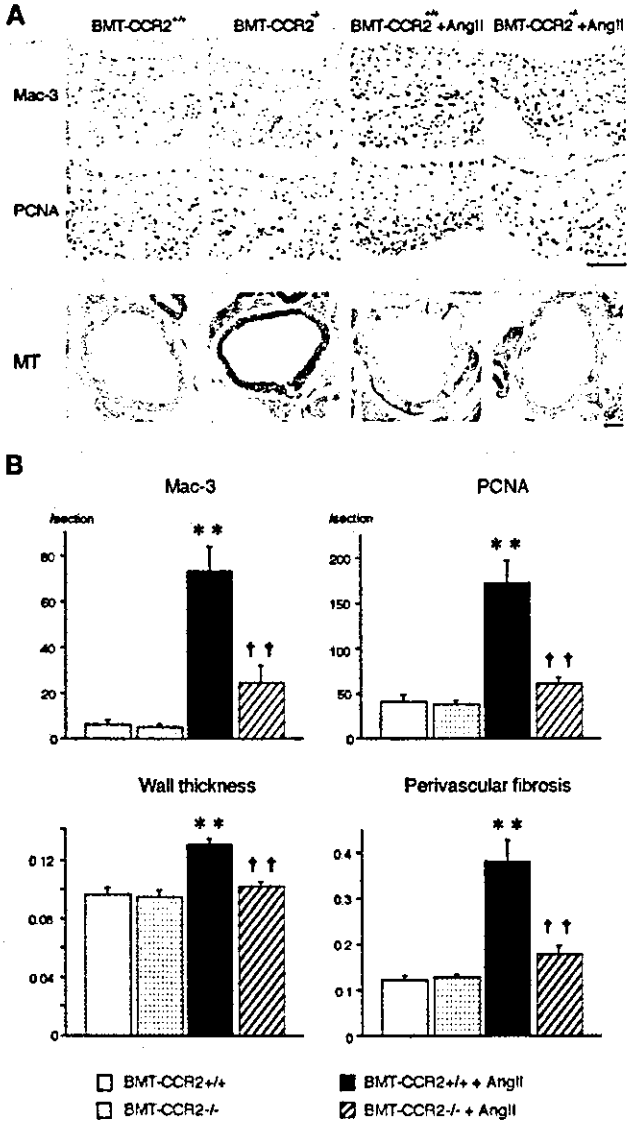

Figure 4. Blunted Ang II-induced inflammation and vascular remodeling in BMT-CCR2$^{-/-}$ mice. A, Aortic cross sections were immunohistochemically stained for macrophages (Mac-3) or a marker of proliferation (PCNA) on day 28. Aortic sections stained with Masson's trichrome on day 28 are also presented (bar=100 μm). B, Number of macrophages infiltrated into the aorta and appearance of proliferating cells in the BMT-CCR2$^{+/+}$, BMT-CCR2$^{-/-}$, BMT-CCR2$^{+/+}$+Ang II, and BMT-CCR2$^{-/-}$+Ang II mice of day 28 of Ang II infusion are shown (positive cell counts per section). Wall thickness (wall-to-lumen ratio) and perivascular fibrosis of the aorta on day 28 are also shown. *P<0.05, **P<0.01 vs BMT-CCR2$^{+/+}$ group; †P<0.05, ††P<0.01 vs BMT-CCR2$^{+/+}$+Ang II group (n=6 each).

without Ang II, suggesting that lesional macrophages might be the major source of CCR2 gene expression in the aortic tissue.

Effects of ARB on CCR2 Expression in Circulating Monocytes in Hypertensive Patients

A pilot clinical study was performed to determine if monocyte CCR2 is enhanced in patients with essential hypertension via AT_1 receptor stimulation. Multivariate analysis revealed that the increased CCR2 intensity on monocytes correlated independently with the presence of hypertension (odds ratio=33.6, 95% confidence interval=4.22≈267.5; P<0.01; Table 2). The monocyte CCR2 intensity in hypertensive patients treated with ARB was similar to that observed in normotensive subjects (Table 1). There were no significant differences in monocyte CCR2 levels in patients treated with different ARB (data not shown). In contrast, there were no significant differences in CXCR2 in neutrophils, or CCR1 in T cells among the three groups (Table 1). There was no significant correlation between the CCR2 intensity on monocytes and the degree of systolic or diastolic hypertension (data not shown).

CCR2 Upregulation in Peripheral Circulating Monocytes of Hypertensive Rats

Monocyte CCR2 intensity was higher in WKY rats made hypertensive with administration of the nitric oxide synthesis inhibitor (L-NAME) for 1 week[23] compared with control

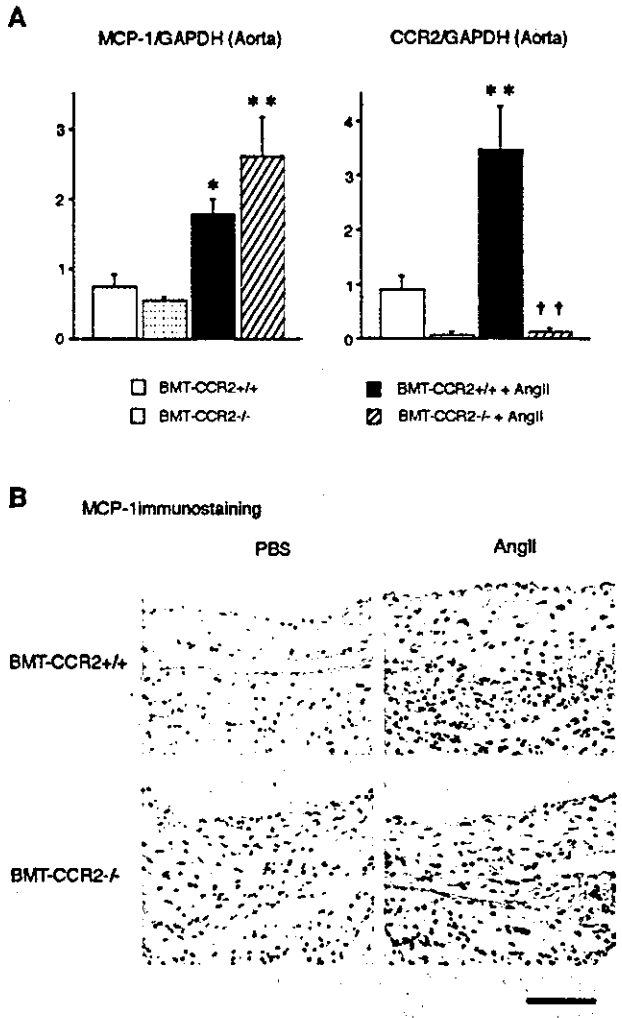

Figure 5. MCP-1 and CCR2 expression of the aorta in BMT mice. A, MCP-1 and CCR2 gene expression by real-time RT-PCR in the aorta on day 28. Data are expressed as the ratio of MCP-1 and CCR2 mRNA to GAPDH mRNA. *P<0.05, **P<0.01 vs BMT-CCR2$^{+/+}$ group; †P<0.05, ††P<0.01 vs BMT-CCR2$^{+/+}$+Ang II group (n=6 each). B, Aortic cross sections were stained immunohistochemically for MCP-1 on day 28 (bar=100 μm).

TABLE 2. Identification of Independent Predictors of the Presence of Hypertension by Multivariate Analysis

Variables	Odds Ratio	95% CI	P
Nonpredictor			
Sex, male	6.02	0.77–47.4	0.40
Age, >70 years	2.24	0.26–19.5	0.47
Smoking	3.49	0.41–29.5	0.25
Alcohol	0.80	0.11–5.82	0.83
Body mass index, >25	6.46	0.55–75.2	0.14
Hypercholesterolemia			
TC, >220 mg/dL	0.28	0.03–2.63	0.26
HDL-C, <40 mg/dL	0.37	0.44–3.51	0.39
LDL-C, >130 mg/dL	0.88	0.07–11.3	0.92
Diabetes	1.78	0.18–17.9	0.63
MCP-1, <8 ng/mL	0.54	0.10–3.04	0.49
CXCR2/neutrophils, MFI	0.98	0.94–1.01	0.15
CCR/T cells, MFI	0.99	0.74–1.32	0.95
Predictor			
CCR2/monocytes, >130, MFI	33.6	4.22267.5	<0.01

untreated rats. The increase in monocyte CCR2 intensity was prevented by treatment with low and high doses of ARB. Monocyte CCR2 intensity was also enhanced in 12-week old SHR, which was reduced by treatment with low and high doses of ARB (online Table 4).

Discussion

Hypertension-induced mechanical strains on monocytes and endothelial cells activate monocyte function resulting in hyperresponsiveness to inflammatory stimuli and secretion of cytokines and growth factors.[36–38] The novel findings of the present study are that (1) CCR2 expression and function (chemotaxis to MCP-1) are enhanced in circulating monocytes in hypertensive animals through an AT_1 receptor–mediated mechanism, and (2) monocyte CCR2 is critical for monocyte-mediated inflammation and remodeling in Ang II–induced hypertension in mice. Although the precise molecular mechanism underlying AT_1 receptor–mediated overexpression of CCR2 in the monocytes is not known, the present data using the SOD-TG mice suggest the possible involvement of ROS. The involvement of ROS is supported by a recent report by Wang et al[35] who demonstrated that treatment of isolated monocytes with antioxidants reduced homocysteine-induced increases in CCR2.

The pilot clinical study indicating that (1) increased CCR2 on monocytes is an important predictor of the presence of hypertension, and (2) hypertensive patients treated with ARB have reduced levels of monocyte CCR2 suggests potential clinical implications of the present observation in animals. Our present data of (1) identical effects of treatment with low and high doses of ARB on monocyte CCR2 expression in mice and rats, and (2) no significant correlation between blood pressure values and the monocyte CCR2 intensity in patients support the hypothesis that ARB-induced diminished CCR2 expression is not explained solely by the blood pressure–lowering effects of ARB. Therefore, a direct action of Ang II mediated via AT_1 receptors beyond blood pressure lowering might be involved in the pathobiology of enhanced monocyte CCR2 expression and function under hypertensive conditions in vivo.

To dissect the relative pathobiological role of monocytes versus nonmonocyte cells in the arterial wall, we used the BMT technique. The most important finding of this study was blunted Ang II–induced aortic inflammation and remodeling in BMT-CCR2$^{-/-}$ mice as well as in CCR2$^{-/-}$ mice. In contrast, cardiac hypertrophy developed in both CCR2$^{-/-}$ and BMT-CCR2$^{-/-}$ mice. The present study therefore provides direct evidence that increased CCR2 expression on monocytes is critical for the development of vascular inflammation and remodeling, but not for left ventricular hypertrophy, in Ang II–induced hypertension. It is plausible therefore that suppression of Ang II–induced vascular remodeling by leukocyte-selective CCR2 deficiency may be the result of reduced recruitment and activation of monocytes. Activated leukocytes might produce growth-promoting signals, which in turn lead to vascular remodeling in a CCR2-deficiency manner. In contrast, Roque et al[30] suggested that upregulation of MCP-1 is responsible for attenuating neointimal smooth muscle growth after arterial injury in CCR2$^{-/-}$ mice. Although there was no detectable difference in Ang II–induced local MCP-1 expression between BMT-CCR2$^{+/+}$ and -CCR2$^{-/-}$ mice, it is possible that some of inhibitory effects seen in BMT-CCR2$^{-/-}$ mice might be related to direct inhibitory effects of MCP-1. The blunted Ang II–induced inflammation and vascular remodeling in BMT-CCR2$^{-/-}$ mice cannot be explained by nonspecific action of irradiation, because (1) Ang II–induced structural changes in the aorta and heart were similar between CCR2$^{+/+}$ and BMT-CCR2$^{+/+}$ mice and (2) Ang II–induced increases in gene and protein expression of MCP-1 were noted in CCR2$^{-/-}$ and BMT-CCR2$^{-/-}$ mice. In conclusion, the present study provides solid evidence that CCR2 expressed on monocytes has a critical role in vascular inflammation and remodeling in Ang II–induced hypertension. This finding might also apply to the pathology of vascular remodeling due to other types of hypertension, because enhanced CCR2 expression and its inhibition by ARB treatment was demonstrated in other types of hypertensive animals and in hypertensive patients. The present data suggest that CCR2-mediated monocyte inflammation is a reasonable target of therapy for treatment of vascular remodeling. Also, blockade of Ang II signals by ARB might act as antiinflammatory therapy beyond blood pressure lowering.

Acknowledgments

This study was supported by Grants-in-Aid for Scientific Research (14657172, 14207036) from the Ministry of Education, Culture, Sports, Science and Technology, Tokyo, Japan, by Health Science Research Grants (Comprehensive Research on Aging and Health, and Research on Translational Research) from the Ministry of Health Labor and Welfare, Tokyo, Japan, and by the Program for Promotion of Fundamental Studies in Health Sciences of the Organization for Pharmaceutical Safety and Research, Tokyo, Japan.

References

1. Dzau VJ. Theodore Cooper lecture. Tissue angiotensin and pathobiology of vascular disease: a unifying hypothesis. *Hypertension.* 2001;37: 1047–1052.

2. Alexander RW. Theodore Cooper memorial lecture. Hypertension and the pathogenesis of atherosclerosis: oxidative stress and the mediation of arterial inflammatory response: a new perspective. *Hypertension.* 1995; 25:155–161.
3. Egashira K. Clinical importance of endothelial function in arteriosclerosis and ischemic heart disease. *Circ J.* 2002;66:529–533.
4. Yusuf S, Sleight P, Pogue J, Bosch J, Davies R, Dagenais G. Effects of an angiotensin-converting-enzyme inhibitor, ramipril, on cardiovascular events in high-risk patients: the heart outcomes prevention evaluation study investigators. *N Engl J Med.* 2000;342:145–153.
5. Pitt B, Poole-Wilson PA, Segal R, Martinez FA, Dickstein K, Camm AJ, Konstam MA, Riegger G, Klinger GH, Neaton J, Sharma D, Thiyagarajan B. Effect of losartan compared with captopril on mortality in patients with symptomatic heart failure: randomised trial–the losartan heart failure survival study elite II. *Lancet.* 2000;355:1582–1587.
6. Cohn JN, Tognoni G. A randomized trial of the angiotensin-receptor blocker valsartan in chronic heart failure. *N Engl J Med.* 2001;345: 1667–1675.
7. Hernandez-Presa M, Bustos C, Ortego M, Tunon J, Renedo G, Ruiz-Ortega M, Egido J. Angiotensin-converting enzyme inhibition prevents arterial nuclear factor-κB activation, monocyte chemoattractant protein-1 expression, and macrophage infiltration in a rabbit model of early accelerated atherosclerosis. *Circulation.* 1997;95:1532–1541.
8. Chen XL, Tummala PE, Olbrych MT, Alexander RW, Medford RM. Angiotensin II induces monocyte chemoattractant protein-1 gene expression in rat vascular smooth muscle cells. *Circ Res.* 1998;83: 952–959.
9. Gerard C, Rollins BJ. Chemokines and disease. *Nat Immunol.* 2001;2: 108–115.
10. Mukaida N, Harada A, Matsushima K. Interleukin-8 (IL-8) and monocyte chemotactic and activating factor (mcaf/mcp-1), chemokines essentially involved in inflammatory and immune reactions. *Cytokine Growth Factor Rev.* 1998;9:9–23.
11. Egashira K. Molecular mechanisms mediating inflammation in vascular disease: special reference to monocyte chemoattractant protein-1. *Hypertension.* 2003;41:834–841.
12. Capers Qt, Alexander RW, Lou P, De Leon H, Wilcox JN, Ishizaka N, Howard AB, Taylor WR. Monocyte chemoattractant protein-1 expression in aortic tissues of hypertensive rats. *Hypertension.* 1997;30:1397–1402.
13. Usui M, Egashira K, Tomita H, Koyanagi M, Katoh M, Shimokawa H, Takeya M, Yoshimura T, Matsushima K, Takeshita A. Important role of local angiotensin II activity mediated via type 1 receptor in the pathogenesis of cardiovascular inflammatory changes induced by chronic blockade of nitric oxide synthesis in rats. *Circulation.* 2000;101:305–310.
14. Jiang Y, Beller DI, Frendl G, Graves DT. Monocyte chemoattractant protein-1 regulates adhesion molecule expression and cytokine production in human monocytes. *J Immunol.* 1992;148:2423–2428.
15. Viedt C, Vogel J, Athanasiou T, Shen W, Orth SR, Kubler W, Kreuzer J. Monocyte chemoattractant protein-1 induces proliferation and interleukin-6 production in human smooth muscle cells by differential activation of nuclear factor-κB and activator protein-1. *Arterioscler Thromb Vasc Biol.* 2002;22:914–920.
16. Schecter AD, Rollins BJ, Zhang YJ, Charo IF, Fallon JT, Rossikhina M, Giesen PL, Nemerson Y, Taubman MB. Tissue factor is induced by monocyte chemoattractant protein-1 in human aortic smooth muscle and THP-1 cells. *J Biol Chem.* 1997;272:28568–28573.
17. Mori E, Komori K, Yamaoka T, Tanii M, Kataoka C, Takeshita A, Usui M, Egashira K, Sugimachi K. Essential role of monocyte chemoattractant protein-1 in development of restenotic changes (neointimal hyperplasia and constrictive remodeling) after balloon angioplasty in hypercholesterolemic rabbits. *Circulation.* 2002;105:2905–2910.
18. Usui M, Egashira K, Ohtani K, Kataoka C, Ishibashi M, Hiasa K, Katoh M, Zhao Q, Kitamoto S, Takeshita A. Anti-monocyte chemoattractant protein-1 gene therapy inhibits restenotic changes (neointimal hyperplasia) after balloon injury in rats and monkeys. *FASEB J.* 2002;16: 1838–1840.
19. Namiki M, Kawashima S, Yamashita T, Ozaki M, Hirase T, Ishida T, Inoue N, Hirata K, Matsukawa A, Morishita R, Kaneda Y, Yokoyama M. Local overexpression of monocyte chemoattractant protein-1 at vessel wall induces infiltration of macrophages and formation of atherosclerotic lesion: synergism with hypercholesterolemia. *Arterioscler Thromb Vasc Biol.* 2002;22:115–120.
20. Aiello RJ, Bourassa PA, Lindsey S, Weng W, Natoli E, Rollins BJ, Milos PM. Monocyte chemoattractant protein-1 accelerates atherosclerosis in apolipoprotein E–deficient mice. *Arterioscler Thromb Vasc Biol.* 1999; 19:1518–1525.
21. Koyanagi M, Egashira K, Kitamoto S, Ni W, Shimokawa H, Takeya M, Yoshimura T, Takeshita A. Role of monocyte chemoattractant protein-1 in cardiovascular remodeling induced by chronic blockade of nitric oxide synthesis. *Circulation.* 2000;102:2243–2248.
22. Kitamoto S, Egashira K, Kataoka C, Koyanagi M, Katoh M, Shimokawa H, Morishita R, Kaneda Y, Sueishi K, Takeshita A. Increased activity of nuclear factor-κB participates in cardiovascular remodeling induced by chronic inhibition of nitric oxide synthesis in rats. *Circulation.* 2000;102: 806–812.
23. Takemoto M, Egashira K, Usui M, Numaguchi K, Tomita H, Tsutsui H, Shimokawa H, Sueishi K, Takeshita A. Important role of tissue angiotensin-converting enzyme activity in the pathogenesis of coronary vascular and myocardial structural changes induced by long-term blockade of nitric oxide synthesis in rats. *J Clin Invest.* 1997;99:278–287.
24. Egashira K, Zhao Q, Kataoka C, Ohtani K, Usui M, Charo IF, Nishida K, Inoue S, Katoh M, Ichiki T, Takeshita A. Importance of monocyte chemoattractant protein-1 pathway in neointimal hyperplasia after periarterial injury in mice and monkeys. *Circ Res.* 2002;90:1167–1172.
25. Boring L, Gosling J, Cleary M, Charo IF. Decreased lesion formation in CCR2−/− mice reveals a role for chemokines in the initiation of atherosclerosis. *Nature.* 1998;394:894–897.
26. Gu L, Okada Y, Clinton SK, Gerard C, Sukhova GK, Libby P, Rollins BJ. Absence of monocyte chemoattractant protein-1 reduces atherosclerosis in low density lipoprotein receptor-deficient mice. *Mol Cell.* 1998;2: 275–281.
27. Ni W, Egashira K, Kitamoto S, Kataoka C, Koyanagi M, Inoue S, Imaizumi K, Akiyama C, Nishida Ki K, Takeshita A. New anti-monocyte chemoattractant protein-1 gene therapy attenuates atherosclerosis in apolipoprotein E–knockout mice. *Circulation.* 2001;103:2096–2101.
28. Inoue S, Egashira K, Ni W, Kitamoto S, Usui M, Otani K, Ishibashi M, Hiasa K, Nishida K, Takeshita A. Anti-monocyte chemoattractant protein-1 gene therapy limits progression and destabilization of established atherosclerosis in apolipoprotein E–knockout mice. *Circulation.* 2002;106:2700–2706.
29. Ni W, Kitamoto S, Ishibashi M, Usui M, Inoue S, Hiasa K, Zhao Q, Nishida K, Takeshita A, Egashira K. Monocyte chemoattractant protein-1 is an essential inflammatory mediator in angiotensin II–induced progression of established atherosclerosis in hypercholesterolemic mice. *Arterioscler Thromb Vasc Biol.* 2004;24:534–539.
30. Roque M, Kim WJ, Gazdoin M, Malik A, Reis ED, Fallon JT, Badimon JJ, Charo IF, Taubman MB. CCR2 deficiency decreases intimal hyperplasia after arterial injury. *Arterioscler Thromb Vasc Biol.* 2002;22: 554–559.
31. Bush E, Maeda N, Kuziel WA, Dawson TC, Wilcox JN, DeLeon H, Taylor WR. CC chemokine receptor 2 is required for macrophage infiltration and vascular hypertrophy in angiotensin II–induced hypertension. *Hypertension.* 2000;36:360–363.
32. Sugaya T, Nishimatsu S, Tanimoto K, Takimoto E, Yamagishi T, Imamura K, Goto S, Imaizumi K, Hisada Y, Otsuka A, Uchida H, Sugiura M, Fukuta K, Fukamizu A, Murakami K. Angiotensin II type 1a receptor-deficient mice with hypotension and hyperreninemia. *J Biol Chem.* 1995; 270:18719–18722.
33. Sata M, Saiura A, Kunisato A, Tojo A, Okada S, Tokuhisa T, Hirai H, Makuuchi M, Hirata Y, Nagai R. Hematopoietic stem cells differentiate into vascular cells that participate in the pathogenesis of atherosclerosis. *Nat Med.* 2002;8:403–409.
34. Han KH, Tangirala RK, Green SR, Quehenberger O. Chemokine receptor CCR2 expression and monocyte chemoattractant protein-1-mediated chemotaxis in human monocytes: a regulatory role for plasma LDL. *Arterioscler Thromb Vasc Biol.* 1998;18:1983–1991.
35. Wang G, O K. Homocysteine stimulates the expression of monocyte chemoattractant protein-1 receptor (CCR2) in human monocytes: possible involvement of oxygen free radicals. *Biochem J.* 2001;357:233–240.
36. Liu Y, Liu T, McCarron RM, Spatz M, Feuerstein G, Hallenbeck JM, Siren AL. Evidence for activation of endothelium and monocytes in hypertensive rats. *Am J Physiol.* 1996;270:H2125–H2131.
37. Han KH, Han KO, Green SR, Quehenberger O. Expression of the monocyte chemoattractant protein-1 receptor CCR2 is increased in hypercholesterolemia: differential effects of plasma lipoproteins on monocyte function. *J Lipid Res.* 1999;40:1053–1063.
38. Ishibashi M, Egashira K, Hiasa K, Inoue S, Ni W, Zhao Q, Usui M, Kitamoto S, Ichiki T, Takeshita A. Antiinflammatory and antiarteriosclerotic effects of pioglitazone. *Hypertension.* 2002;40:687–693.

Gene Therapy (2004) 11, 1273–1282

www.nature.com/gt

RESEARCH ARTICLE

Antimonocyte chemoattractant protein-1 gene therapy reduces experimental in-stent restenosis in hypercholesterolemic rabbits and monkeys

K Ohtani[1], M Usui[1], K Nakano[1], Y Kohjimoto[2], S Kitajima[2], Y Hirouchi[2], X-H Li[3], S Kitamoto[1], A Takeshita[1] and K Egashira[1]

[1]*Department of Cardiovascular Medicine, Graduate School of Medical Sciences, Kyushu University, Fukuoka, Japan;* [2]*Primate Research Center, Guandong, China; and* [3]*Gaoyao Kangda Laboratory Animals Science and Technology, Guandong, China*

In-stent restenosis results exclusively from neointimal hyperplasia due to mechanical injury and a foreign body response to the prosthesis. Inflammation mediated by monocyte chemoattractant protein-1 (MCP-1) might therefore underlie in-stent restenosis. We recently devised a new strategy for anti-MCP-1 gene therapy by transfecting an N-terminal deletion mutant of the MCP-1 gene into skeletal muscles. We used this strategy to investigate the role of MCP-1 in experimental in-stent restenosis in hypercholesterolemic rabbits and monkeys. Transfection of the mutant MCP-1 gene suppressed monocyte infiltration/activation in the stented arterial wall and markedly reduced the development of neointimal hyperplasia. This strategy also suppressed local expression of MCP-1 and inflammatory cytokines. Therefore, inhibition of MCP-1-mediated inflammation is effective in reducing experimental in-stent restenosis. This strategy might be a useful form of gene therapy against human in-stent restenosis.
Gene Therapy (2004) **11**, 1273–1282. doi:10.1038/sj.gt.3302288; Published online 3 June 2004

Keywords: *monocyte; inflammation; restenosis; stent*

Introduction

Each year, more than 1.5 million patients undergo percutaneous coronary intervention of atherothrombotic lesions worldwide. Stent implantation is now the major revascularization technique.[1] Although the stent technique reduces the restenosis rate in selected coronary artery lesions, restenosis continues to occur in high-risk lesions or patients, and thus still remains an unsolved clinical issue. Anatomically, in-stent restenosis results exclusively from neointimal hyperplasia, whereas restenosis after balloon angioplasty results from neointimal hyperplasia and negative remodeling of the arterial wall.[2] There is a two-fold greater incidence of neointimal hyperplasia after stent implantation than after balloon angioplasty.[3] Recent evidence suggests that in addition to mechanical injury, an intense foreign body response to stent prosthesis induces acute and chronic inflammation in the arterial wall, ensuing production of cytokines and growth factors that subsequently induce proliferation and migration of vascular smooth muscle cells.[3,4,5] Experimental and clinical data suggest that inhibition of cellular proliferation with sirolimus might be an effective strategy to suppress in-stent restenosis.[6–9]

There is growing evidence from clinical and animal studies indicating that inflammation is a central mediator in restenosis.[10–12] Recruitment and activation of monocytes/macrophages are major early histopathologic findings after arterial injury. As monocyte chemoattractant protein-1 (MCP-1) is a potent and specific chemokine for monocytes,[13,14] an anti-inflammatory strategy targeting MCP-1 and its receptor (CCR2) might be an appropriate and reasonable approach for the treatment of restenosis. We recently devised a new strategy for anti-MCP-1 gene therapy by transfecting plasmid cDNA encoding a mutant MCP-1 gene into skeletal muscle.[15] This mutant MCP-1 lacks N-terminal amino acids 2–8, called 7ND, forms inactive heterodimers with wild-type MCP-1, and thus works as a dominant-negative inhibitor of MCP-1.[16] This method (intramuscular (i.m.) transfection of the gene) is useful because direct gene transfer into the injured arterial wall is not necessary and the role of MCP-1 can be investigated under pathophysiologic conditions *in vivo*. We used this strategy to demonstrate that blockade of the MCP-1 signal reduces neointimal hyperplasia after injury[17,18,19] and atherosclerosis.[20,21] Roque *et al*[22] reported reduced neointimal hyperplasia after intraluminal arterial injury in CCR2-deficient mice. With regard to the role of MCP-1 in in-stent restenosis, Horvath *et al*[23] demonstrated that blockade of the MCP-1 receptor (CCR2) with anti-CCR2 antibody reduced neointimal hyperplasia by 40% after stenting by inhibiting monocyte infiltration in normocholesterolemic monkeys. In the latter study, however, the efficacy of CCR2 blockade might have been limited due to possible antigenic actions from the use of murine antibody in monkeys. Furthermore, because of the use of

Correspondence: Dr K Egashira, Department of Cardiovascular Medicine, Graduate School of Medical Science, Kyushu University, 3-1-1, Maidashi, Higashi-ku, Fukuoka 812-8582, Japan
Received 12 October 2003; accepted 19 March 2004; published online 3 June 2004

normocholesterolemic monkeys, the degree of stent-induced neointimal hyperplasia was markedly less than that reported in humans and in hypercholesterolemic animals.

Therefore, the primary aim of this study was to test the hypothesis that MCP-1-mediated arterial inflammation is the underlying mechanism in in-stent neointimal hyperplasia in hypercholesterolemic rabbits and monkeys, which might be more clinically relevant animal models than normocholesterolemic animals.[24]

Results

Effects of 7ND gene transfer in rabbits

We measured gene expression of cytokines and chemokines 7 days after stenting (Figure 1a) (Table 1). The mRNA levels of interleukin (IL)-6, tissue necrosis factor (TNF)α, IL-1β, matrix metalloproteinases (MMP)-2, MMP-9, and vascular endothelial growth factor (VEGF) were higher in the stented artery than in the noninjured normal control artery. 7ND gene transfer did not affect the increase in mRNA levels of TNFα, MMP-2, and MMP-9, but reduced the increases in IL-6, IL-1β, and VEGF levels. We immunohistochemically examined MCP-1 and VEGF expression and found that immunoreactive MCP-1 and VEGF increased 7 days after stenting (Figures 1b and c). Minor MCP-1 or VEGF immunostaining was detected in the noninjured control artery, whereas there was intense MCP-1 and VEGF immunoreactivity mainly in the media and intima 7 days after stenting. 7ND gene transfer markedly reduced the magnitude of MCP-1 and VEGF immunostaining (Figures 1b and c).

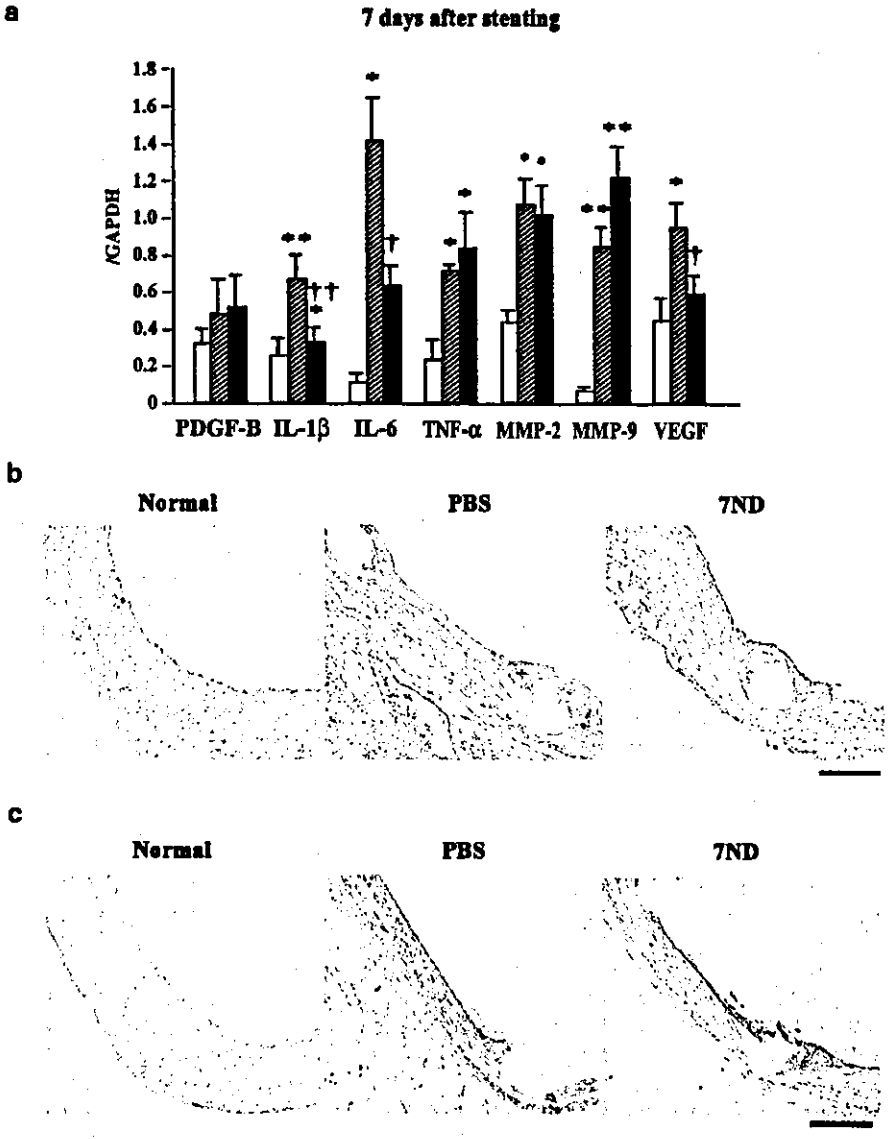

Figure 1 *Gene expression and immunohistochemistry in the stented artery of rabbits. (a) Analysis of expression of various genes by real-time RT-PCR in noninjured controls (open bars) and stented arteries from PBS-treated rabbits (hatched bars) and stented arteries from rabbits transfected with 7ND gene (closed bars). N=7–8. *P<0.05, **P<0.01 versus control (no injury); †P<0.05, ††P<0.01 versus the PBS group. (b) Arterial sections of control nonstented artery or stented arteries from the PBS-treated and 7ND-transfected group stained immunohistochemically with the antibody against MCP-1 7 days after stenting in rabbits. Bar=200 μm. (c) Effects of 7ND gene transfer on protein expression of VEGF. Noninjured control artery section and stented artery sections from the PBS and 7ND group stained immunohistochemically with the antibody against VEGF. Bar=200 μm.*

Table 1 Probes used for real-time PCR

Assay	*Sequence*	*Acc. no.*
PDGF-B		
Forward	5′-CCCATCTACATCATCACCGAGTAC-3′	AB020215
Reverse	5′-GAGTGCTGCTGCAGGAAGGT-3′	
TaqMan probe	5′-TGGACTACCTGCACCGCAACAAGC-3′	
IL-6		
Forward	5′-CATGGTGCTGAAGAACATCCAA-3′	AF169176
Reverse	5′-ACTGGTTTTTCTGCTGCAGGTT-3′	
TaqMan probe	5′-AATGAAGAAGCCACCCTCAAGCCAGC-3′	
IL-1β		
Forward	5′-TCAGCACCTCTCAGACAGAGTACAT-3′	M26295
Reverse	5′-AAGACACGAATTCCATGCTGAA-3′	
TaqMan probe	5′-AAACAACAGTGGCGGCCAAGACCTAA-3′	
TNF-α		
Forward	5′-CATGGTGCTGAAGAACATCCAA-3′	M12845
Reverse	5′-ACTGGTTTTTCTGCTGCAGGTT-3′	
TaqMan probe	5′-AATGAAGAAGCCACCCTCAAGCCAGC-3′	
MMP-2		
Forward	5′-GGAGAAGGCCGTGTTCTTTG-3′	D63579
Reverse	5′-CAGTTGAAGGCCGCGTCTAC-3′	
TaqMan probe	5′-CCAAGCCTCTGACCAGCCTCGG-3′	
MMP-9		
Forward	5′-GCAGGATGTCAAAGCTCACGTA-3′	D26514
Reverse	5′-AACACACACGACGTCTTCCAGTA-3′	
TaqMan probe	5′-TCACACGCCAGAAGAAGCGGTCC-3′	
VEGF		
Forward	5′-GGCTGCTGCAATGATGAAAG-3′	AB020216
Reverse	5′-TTGATCCGCATGATCTGCAT-3′	
TaqMan probe	5′-TGCCCACCGAGGAGTTCAACGTC-3′	
GAPDH		
Forward	5′-CTCTGGCAAAGTGGATGTTGTC-3′	L23961
Reverse	5′-GGGTGGAATCATACTGGAACATG-3′	
TaqMan probe	5′-CCATCAATGATCCATTCATTGACCTCCA-3′	

Acc. no. indicates the accession number in GenBank.

Vascular inflammation, proliferation, and apoptotic cell death were examined 7 days after stent implantation. Infiltration of monocytes/macrophages (Figure 2a) and appearance of proliferating cells (Figure 2b) were observed in the intima and media. Apoptotic cells (Figure 2c) were observed in the intima. Increased inflammation, proliferation, and apoptotic cell death persisted mainly in the neointima at 28 days (data not shown). 7ND gene transfer attenuated the inflammation and proliferation, and enhanced cell death after stenting (Figure 2). There were equal numbers of endothelial cells, monitored by CD31 immunoreactivity in animals treated with phosphate-buffered saline (PBS) or transfected with 7ND gene (Figure 2d). Neointimal hyperplasia was examined by intravascular ultrasound (IVUS) and by histopathologic analysis 28 days after stenting (Figure 3). We detected significant neointimal hyperplasia 28 days after stenting in the PBS-treated rabbits. 7ND gene transfer markedly reduced the neointimal formation as assessed by ultrasonographic and histologic analyses (Figure 3).

We measured plasma and femoral muscle concentrations of 7ND after 7ND or empty plasmid transfection. Plasma 7ND was detected in the plasma 3, 7, and 14 days after 7ND transfection (Table 2). On day 3 of transfection, 7ND could be detected only in 7ND-transfected muscle (Table 3). These data confirm that 7ND protein was released from transfected muscles to circulation.

Effects of 7ND gene transfer in monkeys

Histopathologic and immunohistochemical analyses were performed 28 days after stenting (Figure 4). MCP-1 immunoreactivity was not detected in the nonstented artery (data not shown), whereas intense MCP-1 and CCR2 immunoreactivity was evident mainly in the neointima around the stent prosthesis and weakly in the media (Figure 4a). As seen in rabbits, 7ND gene transfer reduced the magnitude of MCP-1 immunostaining (data not shown) and the neointimal formation (Figures 4b and c).

Effects of 7ND gene transfer in cholesterol levels

In rabbits, the total cholesterol levels before and 28 days after stenting were 922 ± 108 and 968 ± 166 mg/dl in the PBS-treated group, and 938 ± 74 and 950 ± 117 mg/dl in 7ND-transfected group. In monkeys, the total cholesterol

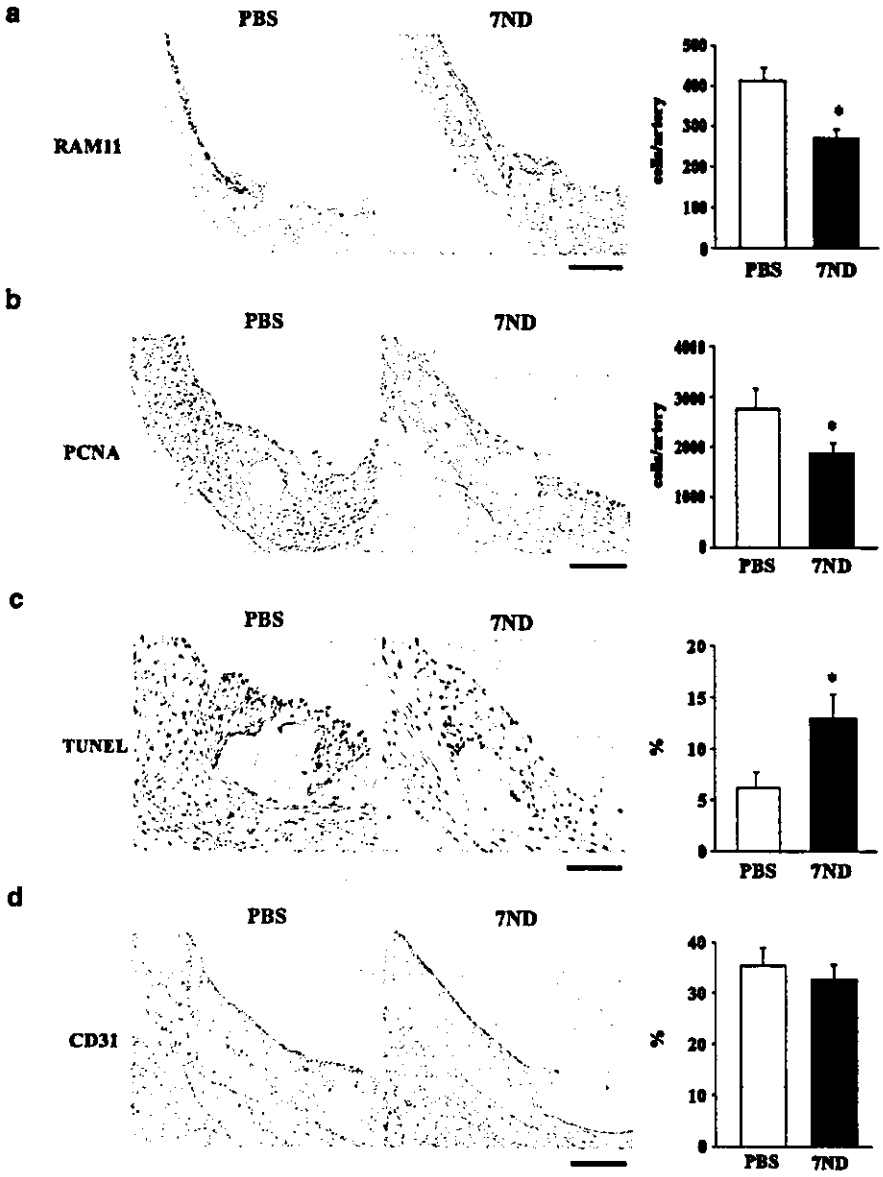

*Figure 2 Inflammation, proliferation, and cell death in the stented artery of rabbits. (a) Effects of 7ND gene transfer on inflammatory changes. Artery sections 7 days after stenting from a rabbit transfected with PBS and a rabbit transfected with 7ND plasmid immunohistochemically stained for monocytes /macrophages (RAM11) and summary of quantitative analyses are presented (n = 8 each). *P < 0.01 versus PBS. Bar = 200 μm. (b) Effects of 7ND gene transfer on proliferative changes. Artery sections 7 days after stenting immunohistochemically stained for PCNA and summary of quantitative analyses are presented (n = 8 each). *P < 0.01 versus PBS. Bar = 200 μm. (c) Effects of 7ND gene transfer on cell death. TUNEL-stained artery sections 7 days after stenting and summary of quantitative analyses are presented (n = 8 each). *P < 0.05 versus PBS. Bar, 100 μm. (d) Effects of 7ND gene transfer on CD31-positive endothelial lining 7 days after stenting and summary of quantitative analyses are presented (n = 8 each). Bar, 100 μm.*

levels before and 28 days after stenting were 444 ± 43 and 429 ± 37 mg/dl in the PBS-treated group, and 469 ± 30 and 488 ± 44 mg/dl in 7ND-transfected group. These data indicate that the observed effects of 7ND gene transfer were not due to changes in serum cholesterol levels.

Antibody production in 7ND-transfected monkeys

In ELISA assay, IgG and IgM antibodies against 7ND protein were not detected after 7ND transfection ($n = 6$ each, Figure 5).

Discussion

The present study demonstrated that blockade of MCP-1 by 7ND gene transfer attenuated monocyte infiltration, and thus suppressed the development of neointimal formation after stent placement in hypercholesterolemic rabbits and non-human primates (cynomolgus monkeys), indicating a role of MCP-1 in stent-induced experimental restenosis (neointimal formation).

Recent studies suggested that inflammation is an important determinant of in-stent neointimal hyperplasia. Inflammation associated with coronary stenting was

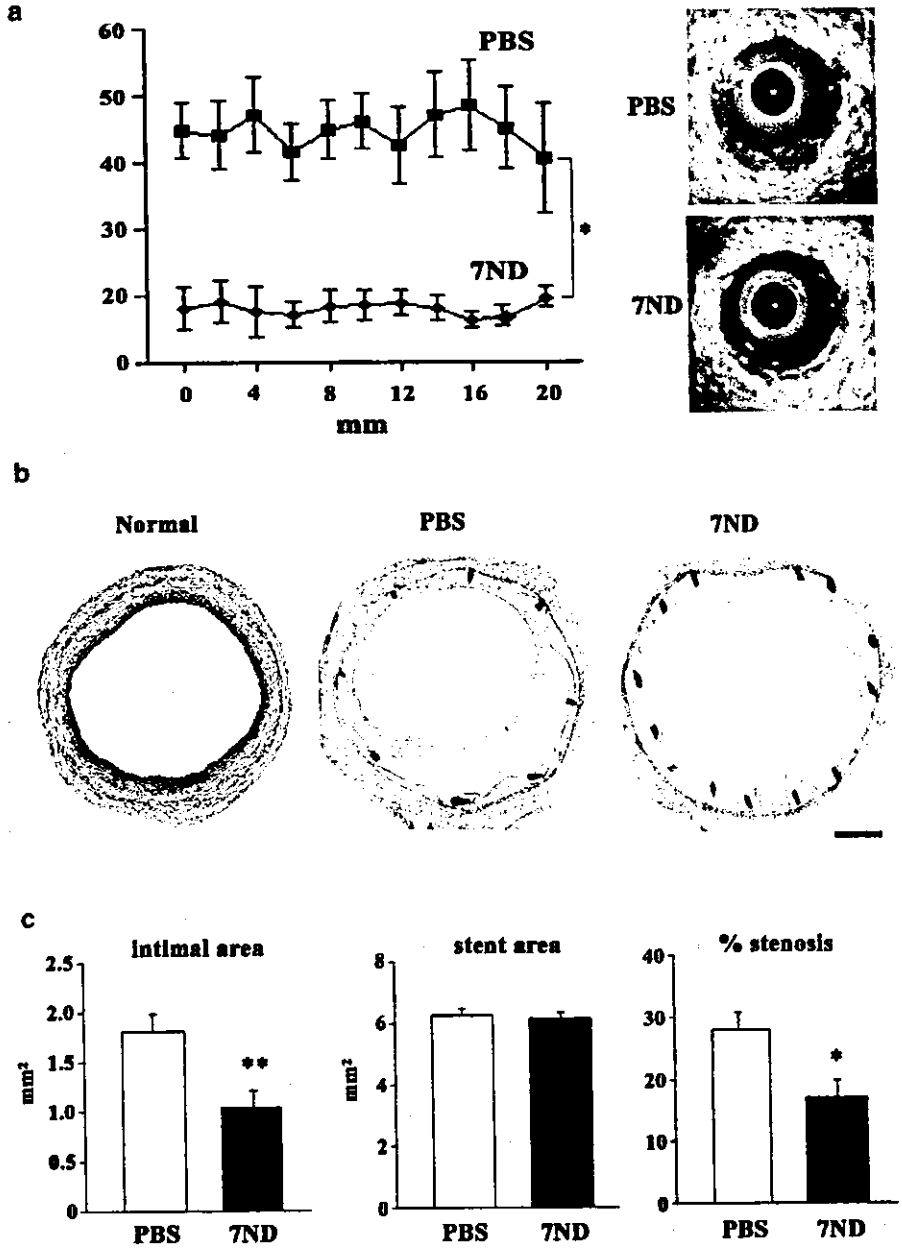

Figure 3 *Effects of 7ND gene transfer on in-stent neointimal hyperplasia in rabbits. (a) Left: mean percent area stenosis within stent in the PBS-treated and 7ND-transfected rabbits as assessed by intravascular ultrasound. X-axis: distance from the distal to the proximal stent end; Y-axis: % cross-sectional stenosis. The upper right panel shows an intravascular ultrasound cross-section image in PBS-treated animal with large neointimal hyperplasia. The lower right panel displays an intravascular ultrasound cross-section image in 7ND-transfected animal with small neointimal hyperplasia. *P<0.01 between PBS and 7ND. (b) Noninjured control artery section (left panel) and artery sections from the PBS-treated group (middle panel) and 7ND-transfected group (right panel) 28 days after stenting stained with elastic van-Gieson in rabbits. Bar=600 μm. (c) Effect of 7ND gene transfer on intimal area, stented area, and % stenosis 28 days after stenting in rabbits (n=8 each). *P<0.05, **P<0.01 versus PBS.*

described previously[3,10]; neutrophils surrounding stent struts are observed only transiently within early stages, whereas chronic inflammatory cells such as monocytes are observed both in early (within 7 days) and late stages (6 months or later) after stenting. Increased monocyte inflammation is associated with greater neointimal formation after stenting in animals[25] and humans.[10] Furthermore, a monoclonal antibody against the adhesion molecule Mac-1 reduced monocyte recruitment and neointimal formation after rabbit iliac artery stenting.[26] As inflammation is unavoidable during stent placement, therapies directed against stent-induced inflammation are a reasonable approach to reduce stent-associated restenosis. Recent experimental studies indicate that a drastic reduction in neointimal formation with rapamycin-eluting stents is mediated by its antiproliferative and anti-inflammatory effects.[6]

There is a rapid increase in plasma MCP-1 within the first day of coronary intervention.[27,28] Persistent increase in MCP-1 after angioplasty is a significant and independent predictor of restenosis.[27] We demonstrated increased immunostaining of MCP-1 after stenting. 7ND gene transfer markedly attenuated inflammatory and proliferative changes and increased apoptotic cell death,

Table 2 Plasma concentrations of 7ND after empty or 7ND plasmid transfection in rabbits

		Days after transfection			
	Baseline	*3*	*7*	*14*	*28*
No transfection (pg/ml)	<20.0 (below detectable limits)	<20.0	<20.0	<20.0	<20.0
Empty plasmid transfection (pg/ml)	<20.0	<20.0	<20.0	<20.0	<20.0
7ND transfection (pg/ml)	<20.0	96±19	76±15	63±9	<20.0

Values are mean±s.e.m., $n=6$–8.

Table 3 Tissue concentrations of 7ND 3 days after empty or 7ND plasmid transfection in rabbits

	Tissue (pg/mg)
No transfection	<20.0
Empty plasmid transfection	<20.0
7ND plasmid transfection	306±39

Values are mean±s.e.m., $n=5$–6.

and thus suppressed in-stent neointimal hyperplasia. Our present data, therefore, suggest that locally produced MCP-1 not only induced the recruitment of monocytes but also activated lesional monocytes and vascular smooth muscle cells to produce the inflammatory cytokines and growth factors (IL-6, IL-1β, VEGF), which in turn might result in in-stent neointimal hyperplasia. We previously reported that 7ND gene transfer suppressed neointimal formation after balloon or cuff injury.[17–19] The present study therefore extends our previous reports with regard to the beneficial effects of 7ND gene transfer on balloon or cuff injury-induced neointimal hyperplasia to in-stent neointimal hyperplasia.

Our finding in non-human primates might have clinical significance, because many therapeutic strategies that have proven effective in reducing restenosis in nonprimate animal model failed to demonstrate a substantial effect on human restenosis. Horvath *et al*[23] demonstrated that injection of an antibody against murine CCR2 attenuated neointimal hyperplasia after iliac arterial stenting in normocholesterolemic cynomolgus monkeys. The magnitude of inflammation and neointimal formation, however, was markedly less in the study by Horvath *et al*[23] (mean intimal thickness in animals with no treatment: 0.25±0.03 mm) than in the present study (0.33±0.02 mm) and those reported in humans[3,10] (0.3–0.5 mm). Small-scale neointimal formation is also reported in normocholesterolemic rabbits (0.13±0.03 mm).[29] This difference might be because hypercholesterolemic animals were used in the present study. Although the appropriate animal model for evaluation of experimental in-stent restenosis is uncertain, the hypercholesterolemic non-human primate model might have an advantage over normocholesterolemic nonprimate animal models, because (1) adequate degrees of neointimal hyperplasia develop after stenting and (2) vascular inflammatory and proliferative responses to injury in non-human primates are presumed to be closer to those in humans than other nonprimate models. Therefore, the use of non-human primates might allow us to evaluate the efficacy of therapies such as 7ND gene transfer on in-stent neointimal hyperplasia under more reliable conditions.

Although this anti-MCP-1 therapy by 7ND gene transfer has yet to be tested for the prevention of restenosis in humans, the beneficial effects observed in rabbit and monkey models suggest a significant potential for this new mode of treatment. For translational research, we must determine as to what is the effective range of 7ND concentration in humans. Basal plasma levels of MCP-1 protein in patients before PCI are reported to be 500 pg/ml.[27] Other reports show plasma MCP-1 levels in patients to be in the range of 150–852 pg/ml.[28,30,31] Compared to plasma MCP-1 levels in humans, 7ND levels achieved by i.m. transfection of 7ND gene in the present study seem to be less. Therefore, further studies are needed to determine the effective range of 7ND concentration in humans before this anti-MCP-1 strategy proceeds to clinical study. As no antibody against 7ND protein was detected after 7ND transfection, it is unlikely that the observed effects of 7ND were due to anti-7ND antibody formation. If this mode of treatment is effective and safe, it could be used as an independent therapy for high-risk lesions, small vessels (<2.5 mm in diameter), or recurrent restenosis. It could also be used as an adjunct therapy for restenosis after drug-eluting stents. 7ND-eluting stents might be associated with a drastic reduction in restenosis in humans.

In conclusion, this study provides evidence that MCP-1-mediated inflammation is an essential mediator in the development of experimental restenosis (neointimal formation) after stenting. Inhibition of stent-associated inflammation by 7ND gene transfer might be a promising next-generation gene therapy to reduce restenosis and to improve clinical outcome after stent placement.

Materials and methods

Plasmid expression vectors

Human 7ND cDNA was constructed by recombinant polymerase chain reaction (PCR) using a wild-type human MCP-1 cDNA (Dr T Yoshimura, National Cancer